

HEAVY-QUARK PHYSICS IN QUANTUM CHROMODYNAMICS*

Stanley J. Brodsky

*Stanford Linear Accelerator Center
Stanford University, Stanford, California 94309*

ABSTRACT

Heavy quarks can expose new symmetries and novel phenomena in QCD not apparent in ordinary hadronic systems. In these lectures I discuss the use of effective-Lagrangian and light-cone Fock methods to analyze exclusive heavy hadron decays such as $\Upsilon \rightarrow p\bar{p}$ and $B \rightarrow \pi\pi$, and also to derive effective Schrödinger and Dirac equations for heavy quark systems. Two contributions to the heavy quark structure functions of the proton and other light hadrons are identified: an "extrinsic" contribution associated with leading twist QCD evolution of the gluon distribution, and a higher twist "intrinsic" contribution due to the hardness of high-mass fluctuations of multi-gluon correlations in hadronic wavefunctions. A non-perturbative calculation of the heavy quark distribution of a meson in QCD in one space and one time is presented. The intrinsic higher twist contributions to the pion and proton structure functions can dominate the hadronic production of heavy quark systems at large longitudinal momentum fraction x_F and give anomalous contributions to the quark structure functions of ordinary hadrons at large x_b . I also discuss a number of ways in which heavy quark production in nuclear targets can test fundamental QCD phenomena and provide constraints on hadronic wavefunctions. The topics include color transparency, finite formation time, and predictions for charm production at threshold, including nuclear-bound quarkonium. I also discuss a number of QCD mechanisms for the suppression of J/ψ and Υ production in nuclear collisions, including gluon shadowing, the peripheral excitation of intrinsic heavy quark components at large x_F , and the coalescence of heavy quarks with co-moving spectators at low x_F . The latter mechanism provides an alternative to quark-gluon plasma explanations for the observed suppression of the J/ψ in heavy-ion collisions.

* Work supported by the Department of Energy contract DE-AC03-76SF00515.

MAST

INTRODUCTION

Although quantum chromodynamics has been extensively tested in its perturbative large momentum transfer regime, many fundamental non-perturbative features of QCD involving confinement and the structure of hadronic wavefunctions remain unexplored. Ideally, one should test a physical theory by varying its basic parameters or by modifying its external conditions. For example, in the case of atomic physics, one can probe the validity of quantum electrodynamics at small length scales by studying muonic atoms, and one can study the induced physical changes in atomic structure by applying external electric and magnetic fields. We also have the ability to change the physical environment and modify the basic parameters of QCD. For example, by studying hadronic production processes in nuclei, we can probe QCD phenomena such as "color transparency," nuclear-induced hadronization, and possible effects due to the formation of a quark-gluon plasma. We can identify non-additive nuclear modifications of structure functions, changes in jet evolution and hadronization, and the various formation times associated with hadronization. Even more important, we can use heavy quark systems to change the basic mass scales of the theory and thus probe QCD in extraordinary ways not possible in ordinary hadrons. In fact, as I shall emphasize in these lectures, the study of the propagation of heavy quark systems in nuclear matter can be used to test a number of interesting features of QCD such as gluon shadowing and anti-shadowing, induced gluon emission, co-mover interactions, and the presence of intrinsic heavy quark Fock states in the wavefunction of ordinary hadrons.

Ideally, one would have hoped to test the heavy quark physics of QCD in toponium ($t\bar{t}$) and other hadrons carrying the top quark. The physics of such systems has been discussed in a comprehensive review by Kuhn and Zerwas.¹ Unfortunately, the present lower limit on the top quark mass $m_t > 89$ GeV from CDF² implies that the top quark will decay before significant QCD binding can occur. Thus QCD studies of heavy particle bound states have to be limited to hadrons containing the charm and beauty quarks.

In QED, the essential physical differences between electronic (e^-Z) and heavy muonic (μ^-Z) atoms is due to the difference in the lepton masses. However, in

QCD, the physical mass scale of light quark systems with $m_q^2 \ll \Lambda_{\overline{MS}}^2$ is set by $\Lambda_{\overline{MS}} \simeq 0.2 \text{ GeV}$, the non-perturbative mass scale of the theory, or the scale associated with chiral symmetry breaking. In the case of heavy quark systems ($Q\bar{Q}$) with $m_Q^2 \gg \Lambda_{\overline{MS}}^2$, chiral symmetry is explicitly broken and the physical scales are primarily determined by m_Q . At low momentum transfers, the form factors and photoproduction of light hadrons are largely ruled by vector meson dominance. In contrast, approximations such as the pole dominance of dispersion relations are "ineffective"³ for heavy quark systems; the form factors of quarkonium are controlled by the quark wavefunctions, just as in atomic physics.

There are other profound differences between light and heavy quark systems in QCD. For example, as noted by Gupta and Quinn,⁴ the QCD hadronization of the final state in e^+e^- annihilation could not lead to standard jet behavior in a world without light quarks, since color-singlet heavy quark hadron formation is perturbatively suppressed by powers of $\alpha_s(m_Q^2)$. In another example, Isgur⁵ has shown that the dominant "nuclear" force between heavy quark hadrons is the exchange force due to quark interchange,⁶ rather than Yukawa meson exchange. (See Fig. 1.) On the other hand, Gribov⁷ has argued that confinement of heavy quarks and gluons would not even occur in QCD without the existence of light quarks.

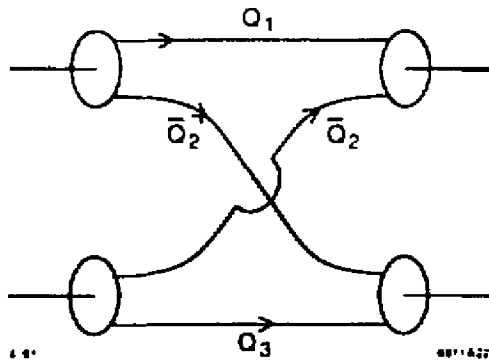


Figure 1 Illustration of the interaction due to the interchange of coninon quarks in meson-meson scattering. The quark interchange amplitude can be computed from the convolution of the four light-cone wavefunctions $\psi_i(x, \vec{k}_{\perp i})$ times the inverse of a light-cone energy denominator. See Ref. 6.

In these lectures I will discuss a number of ways in which heavy quarks simplify QCD physics as well as expose novel phenomena not accessible in ordinary hadrons. For example,

- Since the quark mass acts as a cutoff of final state collinear singularities, jet evolution is calculable in perturbative QCD. Calculations of fragmentation functions to next-to-leading order and di-jet correlation moments for heavy quarks are given in Refs. 8 and 9.
- Since heavy quark systems are effectively non-relativistic $Q\bar{Q}$ bound states, they can be described by an effective single time Schrödinger equation.
- Since the amplitude for gluon emission by heavy quarks is proportional to the quark velocity, the probability for higher Fock states $Q\bar{Q}g$ in the quarkonium rest frame bound-state wavefunction is suppressed by powers of $\Lambda_{\overline{MS}}^2/m_Q^2$.
- In the case of the D and B mesons, the heavy quark acts as a static source whose internal interactions take place over a much shorter time $\tau_Q = \mathcal{O}(m_Q^{-1})$ than the times associated with the bound state scale. Thus, we shall be able to show that such mesons can be described as the bound states of a single-time (radiatively-corrected) Dirac equation for the relativistic light quark.
- As in the case of atomic systems, the hyperfine splitting and other features of the bound state spectrum due to the heavy particle spin is inversely proportional to the heavy quark mass.¹⁰ Furthermore, as emphasized by Lepage and Thacker,¹⁰ Wise and Isgur,¹¹ and others,¹² the physics of the light quark in heavy hadrons $Q\bar{q}$ and Qqq is nearly independent of the heavy quark mass or flavor.
- The effect of virtual heavy quark pairs in light quark systems can be systematically analyzed by effective Lagrangian methods as an expansion in inverse powers of m_Q^2 . The results are analogous to the Serber-Uehling vacuum polarization and non-linear light-by-light scattering corrections in atomic systems.
- Although the probability of intrinsic heavy quark Fock states such as $qqqQ\bar{Q}$ in the wavefunction of ordinary hadrons is suppressed by a power of $\Lambda_{\overline{MS}}^2/m_Q^2$, such wavefunction fluctuations can dominate heavy quark structure functions at large x_b , and lead to anomalous production of heavy quark systems at large x_F .¹³ Thus intrinsic charm and beauty implies not only a hard heavy quark contribution to deep inelastic structure functions but also a

source for quarkonium and heavy hadron production at large x_F in ep and pp collider experiments.^{14,15} An analogous effect for very virtual light-quark pairs, the "intrinsic hardness" of hadronic wavefunctions in QCD may provide a possible explanation of the relatively copious "cumulative production" of hadrons observed at negative x_F in hadron-nucleus collisions.¹⁶

- Because of the large mass scales involved, virtual loop corrections to heavy quark annihilation and decay processes such as $T \rightarrow ggg$ and $T \rightarrow gg\gamma$ can be analyzed in perturbation theory. The argument \hat{Q} of the running coupling constant can be fixed unambiguously by using the method of "automatic scale fixing".¹⁷
- The decay $T \rightarrow \gamma X$ provides an almost pure $C = +$ gluonium source; the shape of its photon spectrum is largely controlled by perturbative QCD.¹⁸
- Since the dominant subprocesses for heavy quark production in hadron collisions are based upon gluon fusion, $gg \rightarrow Q\bar{Q}$ and $gg \rightarrow Q\bar{Q}g$, one can isolate gluon structure functions and study gluonic shadowing and anti-shadowing in nuclear targets. In the case of charm production at very high energies where $x_g < 10^{-4}$ ordinary QCD evolution leads to such high gluon densities that unitarity limits can be exceeded. In this regime gluon distributions reach saturation and higher twist multi-parton processes in the incident hadrons need to be taken into account. (See Fig. 2.) Further discussion may be found in Ref. 19.
- The exclusive decays of heavy systems to a fixed number of light hadrons such as $J/\psi \rightarrow p\bar{p}$ ²⁰ and $B \rightarrow \pi\pi$ can be analyzed using QCD perturbation theory.²¹ In these reactions one is sensitive to moments of the hadron distribution amplitudes $\phi(x, Q)$, the basic valence wavefunction, which control large momentum transfer exclusive reactions.
- Because of the attractive QCD van der Waals potential, it is possible to form nuclear bound quarkonium resonances such as $\eta_c - {}^3He$ in low energy hadron nuclear collisions at the charm threshold.²² The existence of such states would allow the study of the purely gluonic QCD Van der Waals nuclear potential.
- The production of heavy quark systems at threshold allows the study of hadron physics at low relative velocity. For example, the threshold produc-

tion of charm in $p\bar{p}$ collisions could have a profound effect²³ on the elastic $p\bar{p}$ scattering amplitude, accounting for both the strong spin correlation anomaly observed by Krisch *et al.*²⁴ as well as the apparent breakdown of color transparency seen in quasi-elastic $p\bar{p}$ scattering observed by Carroll *et al.*²⁵

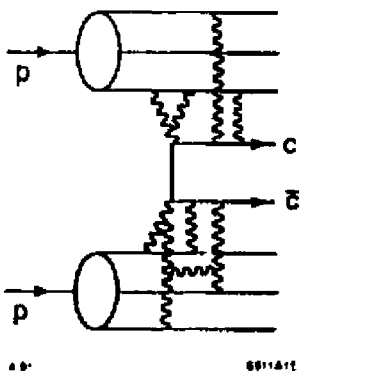


Figure 2 Multi-gluon contribution to charm production in high energy hadron collisions. Such higher twist contributions need to be taken account when the gluon density reaches saturation

One of the most interesting areas of QCD phenomenology is the production of heavy quark systems such as J/ψ , ψ' and the Υ in hadron-nucleus and nucleus-nucleus collisions. The available data are in striking contrast to expectations based on gluon fusion; for example, the J/ψ is produced at large x_F with a rate too large²⁶ to be explained by conventional gluon distributions. In addition, the dependence on nuclear number appears to depend²⁷ on $x_F = x_1 - x_2$ rather than the gluon momentum fraction x_2 in the nucleus as expected from QCD factorization and gluon shadowing. The similarity of the A dependence for the J/ψ and ψ' excludes explanations based on final state absorption of charmonium.

Another remarkable feature of recent data from the E772²⁸ experiment at Fermilab is the suppression of Υ production in proton nucleus collisions at negative x_F in the nuclear fragmentation region. This result suggests that the observations by NA38²⁹ of J/ψ suppression in high transverse energy in heavy ion collisions may not require a specific nucleus-nucleus effect such as color screening by a quark-gluon plasma. In fact, Vogt, Hoyer, and L³⁰ have found that all of the

anomalous features of the data can be accounted for, once one takes into account intrinsic heavy quark Fock components in the initial hadron wavefunction and the effects of heavy quark interactions with the co-moving spectators³¹ that are produced in the nuclear final state. The coalescence of the heavy quarks with the light quark spectators corresponds to “induced hadronization.” For example, capture reactions such as $\bar{q}Q \rightarrow (\bar{q}Q)g$, produce heavy hadrons $Q\bar{q}$ at the expense of quarkonium $Q\bar{Q}$ bound states.

In these lectures I will give a survey of some of the heavy quark phenomena listed above. I will emphasize two main analysis tools, the method of effective Lagrangians^{10,32} which allows one to efficiently catalog heavy quark effects at a given order in $1/m_Q^2$, and the light-cone Fock expansion, which provides a simple representation of hadron wave-functions in terms of their relativistic quark and gluon degrees of freedom.

EFFECTIVE LAGRANGIAN METHODS IN QCD

As I have emphasized in the introduction, heavy quarks can greatly simplify QCD analyses. In the case of heavy hadrons $(\bar{q}Q)$ and (qqQ) , the heavy quark can be treated as a static source with an internal time τ_Q much shorter than the bound state time $\tau_H \sim \Lambda_{MS}^{-1}$. This is immediately apparent in time-ordered perturbation theory where one sees that the leading diagrams have the minimal number of energy denominators involving the heavy quark. Furthermore, the energy transfer to the nucleus $q^0 = q^2/2m_Q$ vanishes in the heavy quark limit.

We thus expect that heavy mesons can be treated in terms of an effective Dirac equation, where the light quark is relativistic, and the heavy quark provides a static source.³³ The physics is even more simplified when one takes into account the fact that the amplitude for the radiation of gluons with physical polarization is of order $g\vec{c} \cdot \vec{p}/m_Q$ and the consequent spin splittings are suppressed for heavy quarks.

The emergence of an effective Dirac equation from the QCD Lagrangian is apparent using effective Lagrangian methods. In general an ultraviolet regulator Λ is needed to define a renormalizable theory such as QCD. In effect all virtual loops are cut-off if $|p^2| > \Lambda^2$. The cut-off Λ is usually taken to be much larger

than all physical scales in the problem. In fact, one is allowed to choose a smaller value for Λ , but at the expense of introducing new power-law suppressed terms in an effective Lagrangian:¹⁰

$$\mathcal{L}^{(\Lambda)} = \mathcal{L}_0^{(\Lambda)}(\alpha_s(\Lambda), m(\Lambda)) + \sum_{n=1}^N \left(\frac{1}{\Lambda}\right)^n \delta\mathcal{L}_n^{(\Lambda)}(\alpha_s(\Lambda), m(\Lambda)) + \mathcal{O}\left(\frac{1}{\Lambda}\right)^{N+1} \quad (1)$$

where

$$\mathcal{L}_0^{(\Lambda)} = -\frac{1}{4} F_{a\mu\nu}^{(\Lambda)} F^{(\Lambda)a\mu\nu} + \bar{\psi}^{(\Lambda)} \left[i\gamma^\mu - m(\Lambda) \right] \psi^{(\Lambda)}. \quad (2)$$

Due to gauge invariance, Lorentz invariance, and other symmetries, there are only a limited number of terms which can contribute at order $1/\Lambda^n$. Furthermore, as emphasized by Lepage and Thacker,¹⁰ the coefficients of each term in $\delta\mathcal{L}_n^{(\Lambda)}$ can be fixed to arbitrary order in $\alpha_s(\Lambda)$ and $m(\Lambda)$ by calculating an appropriate on-shell quark-gluon scattering amplitude to the required order in perturbation theory. As a consequence, all of the physics beyond the scale Λ is replaced by effective (non-renormalizable) local interactions.

As a first example of the use of effective Lagrangians in QCD, let us choose $\Lambda < m_Q$. In this case, all effects of heavy quarks in light quark and gluon hadronic systems are simulated by the effective Lagrangian.

$$\begin{aligned} \delta\mathcal{L}_1^{(\Lambda)} = & -\frac{\alpha_s(\Lambda^2) N_c}{30\pi M_Q^2} D_a F_{\mu\nu}^a D^\mu F_a^{\mu\nu} \\ & + \frac{cg_s^3(\Lambda)}{M_Q^2} F_{\mu\nu}^a F_\tau^{b\nu} F^{c\mu\tau} f_{abc} + \mathcal{O}\left(\frac{1}{M_Q^2}\right). \end{aligned} \quad (3)$$

The first term is equivalent to the Serber-Uehling vacuum polarization correction to low momentum transfer photon exchange in Abelian QED. The second term is special to non-Abelian theories. Since this term couples up to six gluons at order $1/m_Q^2$, it can lead to a significant heavy quark pair content in the non-valence wavefunctions of the proton and other light hadrons. (See Fig. 3.) I return to the phenomenological consequences of this in later sections.

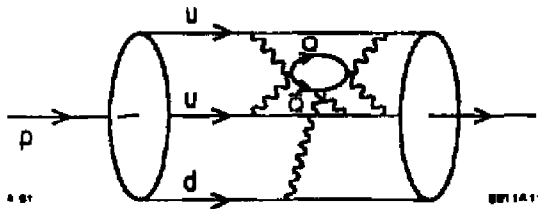


Figure 3. Heavy quark pair fluctuation in the proton wavefunction due to non-Abelian terms in the effective heavy quark Lagrangian at order $1/m_Q^2$

Heavy $Q\bar{Q}$ systems such as the Υ are essentially non-relativistic systems: $\langle r_Q^2 \rangle \sim 1/10$. The probability that the kinetic energy of the massive quark is comparable to its mass is of order $10 \alpha_s^5 < 10^{-3}$. It is thus advantageous to choose Λ slightly larger than m_Q in the effective Lagrangian so that all of the effects of relativistic momenta are restricted to the higher order terms in the effective Lagrangian. In fact, to order $\langle \bar{q}^2 \rangle / \Lambda^2$, the effective Lagrangian for heavy quarks has the form

$$\begin{aligned} \mathcal{L}^{(\Lambda)} &= \mathcal{L}^{(\Lambda)} + \delta\mathcal{L}_1^{(\Lambda)} + \delta\mathcal{L}_2^{(\Lambda)} \\ \delta\mathcal{L}_1^{(\Lambda)} &= \frac{c(\alpha_s, \Lambda) g(\Lambda)}{\Lambda} \bar{\psi} \sigma_{\mu\nu} F^{\mu\nu} \psi \\ \delta\mathcal{L}_2^{(\Lambda)} &= \frac{d(\alpha_s, \Lambda)}{\Lambda^2} \bar{\psi} \gamma_\mu \psi \bar{\psi} \gamma^\mu \psi + \frac{f(\alpha_s, \Lambda)}{\Lambda^2} \bar{\psi} \partial_\mu F^{\mu\nu} \gamma_\nu \psi \dots \end{aligned} \quad (4)$$

where one can use free scattering amplitude calculations to fix the infrared finite coefficients c_i to the desired order in perturbation theory. Furthermore, as shown by Lepage and Caswell,¹⁰ one can now use the Foldy-Wouthuysen transformation to reduce the Lagrangian to two-component spinor form appropriate to heavy quarkonium. The resulting bound state equation is of the Schrödinger form including relativistic, spin, and anomalous moment corrections in the effective potential. An important advantage of this formulation is that one can systematically expand in powers of both \bar{q}^2/m_Q^2 and $K.E./m_Q$ since they are each always small in the bound state equation.

It should also be noted that the effective Lagrangian method can also be applied to heavy mesons $q\bar{Q}$ where only the heavy quark is non-relativistic. In

this case, the heavy quark acts to leading order in $1/m_Q$ as a static source of a non-Abelian QCD potential analogous to the Coulomb potential in muonium ($e^- \mu^+$). Ignoring radiative corrections to the light quark, one thus has

$$[i\partial - gA_{\text{external}}(x) - m_q]\psi_{\text{Dirac}}(x) = 0. \quad (5)$$

More generally, one can correct the Dirac propagator for the light-quark line to include in the Furry picture all of its QCD radiative corrections, as in the Erickson-Yennie formulation of the Lamb Shift of hydrogenic atoms.³⁴ (See Fig. 4.)

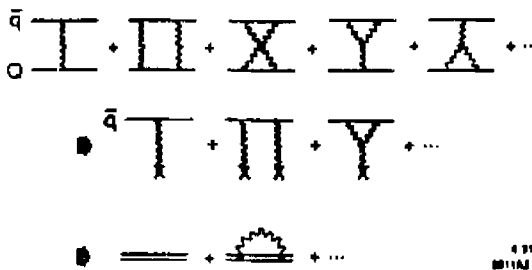


Figure 4 Reduction of the two-particle scattering amplitude for $q\bar{Q} \rightarrow q\bar{Q}$ to single-time Dirac-Furry propagation in the limit where the heavy quark becomes infinitely massive. The double line (Furry propagator) represents the light quark propagating to all orders in the effective (Coulomb-like) static potential of the heavy quark. The equation of motion for the light quark is an effective local Dirac equation modified by QCD radiative corrections.

Notice that by using the effective Lagrangian method, one has effectively reduced the multiple-time Bethe-Salpeter equation formulation of relativistic bound states to an effective single-time Dirac equation which can be systematically improved order by order in $1/m_Q$. It should be emphasized that one must sum an infinite number of crossed graph kernels in the Bethe-Salpeter equation in order to correctly reproduce the physics of the Dirac equation in a Coulomb field.³⁴

The effective Lagrangian method allows one to separate high and low momentum transfer scales for virtually any problem in QCD. In general the physics of virtual corrections from loop momenta $|k^2| > \hat{Q}^2$ is represented by a sum of gauge invariant terms in the local Lagrangian up to the specified order in $1/\hat{Q}^2$.

Because of asymptotic freedom, one can calculate the coefficient functions as a perturbative series in $\alpha_s(\hat{Q}^2)$. By choosing \hat{Q} appropriately, we can calculate any high momentum transfer reaction from the expectation value of the $1/\hat{Q}^2$ term in the effective Lagrangian. There are a number of immediate applications:

- The exclusive decay²¹ of heavy hadrons to light hadrons, such as $B \rightarrow \pi\pi$ in which the weak transition forces internal momentum transfer of order $\hat{Q}^2 = \mu m_B$. Here $\mu^2 \sim \Lambda_{MS}^2$ is a typical hadronic mass scale in QCD.
- Exclusive scattering amplitudes such as hadron form factor $F(Q^2)$.³⁵ These amplitudes involve internal momentum transfers of order $\hat{Q} = cQ$ where c is set by the average momentum fraction of the valence quarks in the hadron wavefunctions.
- Structure functions at the endpoint $x_b \rightarrow 1$. These processes require internal momentum transfers of order $\hat{Q}^2 = -\mu^2/(1-x)$. (See Fig. 5.)
- Exclusive decays of heavy hadrons such as $T \rightarrow p\bar{p}$. These processes involve quark annihilation at the momentum scale $\hat{Q}^2 = m_b^2$.
- Intrinsic heavy quark fluctuations in light hadron wavefunctions. Again these amplitudes require virtual momentum exchange at the scale $\hat{Q}^2 = m_Q^2$.

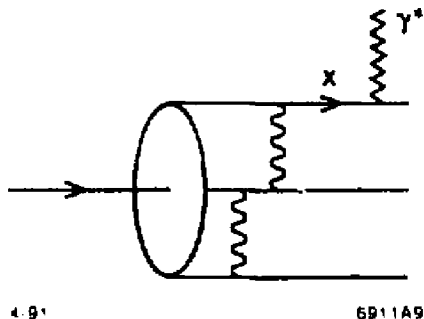


Figure 5. Dominant contribution to the proton structure function at $x_b \rightarrow 1$. Each internal propagator is off shell of order $k^2 \sim -\mu^2/(1-x_b)$.

In these examples, it is easy to verify that the leading order amplitude \mathcal{M} has the leading power behavior set by the dimensional counting rules:³⁵

$$\mathcal{M} = \mathcal{O}[\hat{Q}^{4-n}] \quad (6)$$

where n is the total number of photon, lepton, quark, and gluon fields participating.

ing in the hard scattering. To this order, quark helicity is conserved which leads in turn to hadron helicity conservation in hard exclusive QCD processes.³⁶ In the case of structure functions, one finds that the leading endpoint behavior (before QCD evolution) has the form³⁷

$$G_{q/H}(x) \sim (1-x)^{2n_{\text{spectator}}-1+2\Delta\lambda} \quad (7)$$

where $n_{\text{spectator}}$ is the number of quarks which must be brought to $x = 0$ and $\Delta\lambda$ is the difference between the struck quark and parent hadron's helicity.

In each case, the normalization of the leading amplitude is controlled by the convolution of the corresponding term of the effective Lagrangian with the appropriate bound state hadronic wavefunctions in the low momentum region $|k^2| < \Lambda^2$. We will make this more precise in the next section.

LIGHT-CONE WAVEFUNCTIONS³⁸

As was first emphasized by Dirac³⁹ in 1949, there are many advantages if one quantizes field theories at a fixed time $\tau = t + z/c$ on the light cone rather than at ordinary time t . The primary reason is that boost operators are kinematical rather than dynamical, so that solutions to the bound state problem are automatically obtained for any Lorentz frame. In contrast, in equal-time quantization, calculating the boosted wavefunction is as complicated as diagonalizing the Hamiltonian itself.

In light-cone quantization, a free particle is specified by its four momentum $k^\mu = (k^+, k^-, k_\perp)$ where $k^\pm = k^0 \pm k^3$. Since the particle is on its mass shell and has positive energy, its light-cone energy is also positive: $k^+ = (k_\perp^2 + m^2)/k^+ > 0$. In perturbation theory, transverse momentum $\sum k_\perp$ and the plus momentum $\sum k^+$ are conserved at each vertex. One can construct a complete basis of free Fock states (eigenstates of the free light-cone Hamiltonian) $|n\rangle \langle n| = I$ in the usual way by applying products of free field creation operators to the vacuum

state $|0\rangle$:

$$\begin{aligned}
 & |0\rangle \\
 & |q\bar{q} : \underline{k}_1 \lambda_1 \rangle = b^\dagger(\underline{k}_1 \lambda_1) d^\dagger(\underline{k}_2 \lambda_2) |0\rangle \\
 & |q\bar{q}g : \underline{k}_1 \lambda_1 \rangle = b^\dagger(\underline{k}_1 \lambda_1) d^\dagger(\underline{k}_2 \lambda_2) a^\dagger(\underline{k}_3 \lambda_3) |0\rangle
 \end{aligned} \tag{8}$$

⋮

where b^\dagger , d^\dagger and a^\dagger create bare quarks, antiquarks and gluons having three-momenta \underline{k}_i and helicities λ_i . Of course these "Fock states" are generally not eigenstates of the full Hamiltonian H_{LC} . However the zero-particle state is the only one with zero total P^+ , since all quanta must have positive k^+ , and thus this state cannot mix with the other states in the basis. The free vacuum is thus an exact eigenstate of H_{LC} .

The restriction $k^+ > 0$ is a key difference between light-cone quantization and ordinary equal-time quantization. In equal-time quantization, the state of a parton is specified by its ordinary three-momentum $\vec{k} = (k^1, k^2, k^3)$. Since each component of \vec{k} can be either positive or negative, it is easy to make zero-momentum Fock states that contain particles, and these will mix with the zero-particle state to build up the ground state. In light-cone quantization each of the particles forming a zero-momentum state must have vanishingly small k^+ . Such a configuration represents a point of measure zero in the phase space, and therefore such states can usually be neglected. Actually some care must be taken here since there are operators in the theory that are singular at $k^+ = 0$ —e.g. the kinetic energy $(\vec{k}_\perp^2 + M^2)/k^+$. In certain circumstances, states containing $k^+ \rightarrow 0$ quanta can significantly alter the ground state of the theory. One such circumstance is when there is spontaneous symmetry breaking. Note also that the space of states that play a role in the vacuum structure is much smaller for light-cone quantization than for equal-time quantization; the state of each parton is specified by a two-momentum rather than a three-momentum since $k^+ = 0$. This suggests that vacuum structure may be far simpler to analyze using the light-cone formulation.

The light-cone Fock states form a very useful basis for studying the physical states of the theory. For example, a pion with momentum $\underline{P} \approx (P^+, \vec{P}_\perp)$ is

described by state

$$|\pi : \underline{P}\rangle = \sum_{n, \lambda_i} \int \overline{\prod_i} \frac{dx_i d^2 \vec{k}_{\perp i}}{\sqrt{x_i} 16\pi^3} \left| n : x_i P^+, x_i \vec{P}_\perp + \vec{k}_{\perp i}, \lambda_i \right\rangle \psi_{n/\pi}(x_i, \vec{k}_{\perp i}, \lambda_i) \quad (9)$$

where the sum is over all Fock states and helicities, and where

$$\begin{aligned} \overline{\prod_i} dx_i &\equiv \prod_i dx_i \delta \left(1 - \sum_j x_j \right) \\ \overline{\prod_i} d^2 \vec{k}_{\perp i} &\equiv \prod_i d^2 \vec{k}_{\perp i} 16\pi^3 \delta^2 \left(\sum_i \vec{k}_{\perp i} \right). \end{aligned} \quad (10)$$

The wavefunction $\psi_{n/\pi}(x_i, \vec{k}_{\perp i}, \lambda_i)$ is the amplitude for finding partons with momenta $(x_i P^+, x_i \vec{P}_\perp + \vec{k}_{\perp i})$ in the pion. It does not depend upon the pion's momentum. This special feature of light-cone wavefunctions is not surprising since x_i is the longitudinal momentum fraction carried by the i^{th} -parton ($0 \leq x_i \leq 1$), and $\vec{k}_{\perp i}$ is its momentum "transverse" to the direction of the meson. Both of these are frame independent quantities. The ability to specify wavefunctions simultaneously in any frame is a special feature of light-cone quantization.

In the light-cone Hamiltonian approach, one chooses the light-cone gauge, $\eta \cdot A = A^+ = 0$, for the gluon field. The use of this gauge results in well known simplifications in the perturbative analysis of light-cone dominated processes such as high-momentum hadronic form factors. Furthermore it is indispensable if one desires a simple, intuitive Fock-state basis since there are neither negative-norm gauge boson states nor ghost states in $A^+ = 0$ gauge. Thus each term in the normalization condition

$$\sum_{n, \lambda_i} \int \overline{\prod_i} \frac{dx_i d^2 \vec{k}_{\perp i}}{16\pi^3} |\psi_{n/\pi}(x_i, \vec{k}_{\perp i}, \lambda_i)|^2 = 1 \quad (11)$$

is positive.

Light-Cone Bound-State Equations

Any hadron state, such as $|\pi\rangle$ for the pion, must be an eigenstate of the light-cone Hamiltonian. Consequently, when working in the frame where $P_\pi \equiv (P^+, P_\perp) = (1, 0_\perp)$ and $P_\pi^- = M_\pi^2$, the state $|\pi\rangle$ satisfies an equation

$$(M_\pi^2 - H_{LC}) |\pi\rangle = 0. \quad (12)$$

Projecting this onto the various Fock states $\langle q\bar{q}|$, $\langle q\bar{q}g| \dots$ results in an infinite number of coupled integral eigenvalue equations,

$$\begin{aligned} & \left(M_\pi^2 - \sum_i \frac{\vec{k}_{1i}^2 + m_i^2}{x_i} \right) \begin{bmatrix} \psi_{q\bar{q}/\pi} \\ \psi_{q\bar{q}g/\pi} \\ \vdots \end{bmatrix} \\ &= \begin{bmatrix} \langle q\bar{q} | V | q\bar{q} \rangle & \langle q\bar{q} | V | q\bar{q}g \rangle & \dots \\ \langle q\bar{q}g | V | q\bar{q} \rangle & \langle q\bar{q}g | V | q\bar{q}g \rangle & \dots \\ \vdots & \vdots & \ddots \end{bmatrix} \begin{bmatrix} \psi_{q\bar{q}/\pi} \\ \psi_{q\bar{q}g/\pi} \\ \vdots \end{bmatrix} \end{aligned} \quad (13)$$

where V is the interaction part of H_{LC} . Diagrammatically, V involves completely irreducible interactions — *i.e.*, diagrams having no internal propagators—coupling Fock states. (See Fig. 6.)

$$\begin{bmatrix} \text{Diagram 1} \\ \text{Diagram 2} \\ \vdots \\ \text{...} \end{bmatrix} \begin{bmatrix} \text{Diagram 1} & 0 & \dots \\ 0 & \text{Diagram 2} & \vdots \\ \vdots & \vdots & \ddots \end{bmatrix} \begin{bmatrix} \text{Diagram 1} & \text{Diagram 2} & \dots \\ \text{Diagram 2} & \text{Diagram 1} & \vdots \\ \vdots & \vdots & \ddots \end{bmatrix} \begin{bmatrix} \text{Diagram 1} \\ \text{Diagram 2} \\ \vdots \\ \text{...} \end{bmatrix}$$

Figure 6. Coupled eigenvalue equations for the light-cone wavefunctions of a pion.

These equations determine the hadronic spectrum and wavefunctions. Although the potential is essentially trivial, the many channels required to describe a hadronic state make these equations very difficult to solve. Nevertheless, it is possible to find solutions numerically by diagonalizing the light-cone Hamiltonian in a discrete basis of Fock states obtained by imposing periodic boundary conditions.³⁹ I return to an application of this approach to heavy quarks in the next section.

In principle the hadronic wavefunctions determine all properties of a hadron. The general rule for calculating an amplitude involving wavefunction $\psi_n^{(\Lambda)}$, describing Fock state n in a hadron with $\underline{P} = (P^+, \vec{P}_\perp)$, has the form (see Fig. 7):

$$\sum_{\lambda} \int \prod_i \frac{dx_i d^2 \vec{k}_{\perp i}}{\sqrt{x_i} 16\pi^3} \psi_n^{(\Lambda)}(x_i, \vec{k}_{\perp i}, \lambda_i) T_n^{(\Lambda)}(x, P^+, x, \vec{P}_{\perp} + \vec{k}_{\perp i}, \lambda_i) \quad (14)$$

where $T_n^{(\Lambda)}$ is the irreducible scattering amplitude in LCPT \hbar with the hadron replaced by Fock state n . If only the valence wavefunction is to be used, $T_n^{(\Lambda)}$ is irreducible with respect to the valence Fock state only; e.g. $T_n^{(\Lambda)}$ for a pion has no $q\bar{q}$ intermediate states. Otherwise contributions from all Fock states must be summed, and $T_n^{(\Lambda)}$ is completely irreducible.

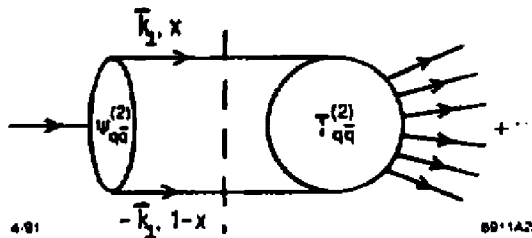


Figure 7 Calculation of hadronic amplitudes in the light-cone Fock formalism

The leptonic decay of the π^\pm is one of the simplest processes to compute since it involves only the $q\bar{q}$ Fock state. The sole contribution to π^+ decay is from

$$\langle 0 | \bar{\psi}_u \gamma^+ (1 - \gamma_5) \psi_d | \pi^- \rangle = -\sqrt{2} P^+ f_\pi$$

$$= \int \frac{dx}{16\pi^3} \frac{d^2 \vec{k}_\perp}{d\vec{u}} \psi_{d\vec{u}}^{(\Lambda)}(x, \vec{k}_\perp) \frac{\sqrt{n_c}}{\sqrt{2}} \left\{ \frac{\bar{v}_1}{\sqrt{1-x}} \gamma^+ (1 - \gamma_5) \frac{u_1}{\sqrt{x}} + (\uparrow \leftrightarrow \downarrow) \right\} \quad (15)$$

where $n_c = 3$ is the number of colors, $f_\pi \approx 93$ MeV, and where only the $L_z = S_z = 0$ component of the general $q\bar{q}$ wavefunction contributes. Thus we have

$$\int \frac{dx d^2 \vec{k}_\perp}{16\pi^3} \psi_{d\vec{k}}^{(\Lambda)}(x, \vec{k}_\perp) = \frac{f_\pi}{2\sqrt{3}}. \quad (16)$$

This result must be independent of the cutoff Λ provided Λ is large compared

with typical hadronic scales. This equation is an important constraint upon the normalization of the $d\bar{u}$ wavefunction. It also shows that there is a finite probability for finding a π^- in a pure $d\bar{u}$ Fock state.

Hadronic Structure Functions and Light-Cone Wavefunctions

In the Bjorken scaling limit, deep inelastic lepton scattering occurs if x_b matches the light-cone fraction of the struck quark. Thus the structure functions can be immediately related to the light-cone probability distributions:

$$2M F_1(x, Q) = \frac{F_2(x, Q)}{x} \approx \sum_a e_a^2 G_{a/p}(x, Q) \quad (17)$$

where

$$G_{a/p}(x, Q) = \sum_{n, \lambda_i} \int \prod_i \frac{dx_i d^2 \vec{k}_{\perp i}}{16\pi^3} |\psi_n^{(Q)}(x_i, \vec{k}_{\perp i}, \lambda_i)|^2 \sum_b \delta(x_b - x) \quad (18)$$

is the number density of partons of type a with longitudinal momentum fraction x in the proton. (The \sum_b is over all partons of type a in Fock state n .) However, the light cone wavefunctions contain much more information for the final state of deep inelastic scattering, including multiparticle distributions, spin and flavor correlations, and the spectator jet composition.

Hadronic Form Factors

The electromagnetic form factor of a pion is defined by the relation

$$\langle \pi : \underline{P}' | J_{em}^\mu | \pi : \underline{P} \rangle = 2(P + P')^\mu F(-(P' - P)^2) \quad (19)$$

where J_{em}^μ is the electromagnetic current operator for the quarks. The form factor is easily expressed in terms of the pion's Fock-state wavefunctions by examining the $\mu = +$ component of this equation in a frame where $\underline{P} = (1, 0)$ and $\underline{P}' = (1, \vec{q}_\perp)$ and $\vec{q}_\perp^2 = Q^2 = -q^2$. Then the spinor algebra is trivial since $\bar{u}(\underline{k}) \gamma^+ u(\underline{l}) =$

$2\sqrt{k+l^+}$, and the form factor is just a sum of overlap integrals analogous to the nonrelativistic formula:⁴⁰ (See Fig. 8.)

$$F(Q^2) = \sum_{n,\lambda} \sum_a e_a \int \prod_i \frac{dx_i d^2 \vec{k}_{\perp i}}{16\pi^3} \psi_n^{(\Lambda)*}(x_i, \vec{k}_{\perp i}, \lambda_i) \psi_n^{(\Lambda)}(x_i, \vec{k}_{\perp i}, \lambda_i). \quad (20)$$

Here e_a is the charge of the struck quark, $\Lambda^2 \gg \vec{q}_\perp^2$, and

$$\vec{l}_{\perp i} \equiv \begin{cases} \vec{k}_{\perp i} - x_i \vec{q}_{\perp i} + \vec{q}_{\perp i} & \text{for the struck quark} \\ \vec{k}_{\perp i} - x_i \vec{q}_{\perp i} & \text{for all other partons.} \end{cases} \quad (21)$$

Notice that the transverse momenta appearing as arguments of the first wavefunction correspond not to the actual momenta carried by the partons but to the actual momenta minus $x_i \vec{q}_{\perp i}$, to account for the motion of the final hadron. Notice also that $\vec{l}_{\perp i}$ and $\vec{k}_{\perp i}$ become equal as $\vec{q}_{\perp i} \rightarrow 0$, and that $F_\pi \rightarrow 1$ in this limit due to wavefunction normalization. The various form factors of hadrons with spin are found by choosing initial and final hadron and helicities.⁴¹

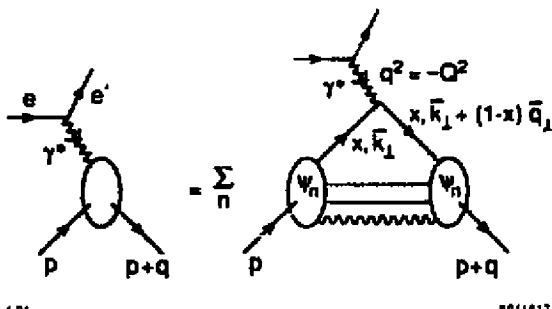


Figure 8. Calculation of the form factor of a bound state from the convolution of light cone Fock amplitudes. The result is exact if one sums over all ψ_n .

Let us now consider the meson form factor at high momentum transfer Q^2 . If the internal momentum transfer exceeds the Lagrangian cut-off Λ then the Drell-Yan convolution of bound state wavefunctions computed from \mathcal{L}_0 does not contribute to $F_M(Q^2)$. In this case the leading contribution is computed from the effective Lagrangian term of order $1/Q^2$. Generally one finds that the amplitudes

for hadron form factors can be written in a factorized form as a convolution of quark distribution amplitudes $\phi(x_i, Q)$, one for each hadron involved in the amplitude, with a hard-scattering amplitude T_H .^{20,42} The pion's electromagnetic form factor, for example, can be written as^{20,42,43}

$$F_\pi(Q^2) = \int_0^1 dx \int_0^1 dy \phi_\pi^*(y, Q) T_H(x, y, Q) \phi_\pi(x, Q) \left(1 + \mathcal{O}\left(\frac{1}{Q}\right) \right). \quad (22)$$

Here T_H is the scattering amplitude for the form factor but with the pions replaced by collinear $q\bar{q}$ pairs—*i.e.* the pions are replaced by their valence partons. We can also regard T_H as the free particle matrix element of the order $1/Q^2$ term in the effective Lagrangian for $\gamma^* q\bar{q} \rightarrow q\bar{q}$.

The process-independent distribution amplitude²⁰ $\phi_\pi(x, Q)$ is the probability amplitude for finding the $q\bar{q}$ pair in the pion with $x_q = x$ and $x_{\bar{q}} = 1 - x$:

$$\phi_\pi(x, Q) = \int \frac{d^2 \vec{k}_\perp}{16\pi^3} \psi_{q\bar{q}/\pi}^!(Q) (x, \vec{k}_\perp) \quad (23)$$

$$= P_\pi^+ \int \frac{dz^-}{4\pi} e^{iz^+ P_\pi^+ z^-/2} \langle 0 | \bar{\psi}(0) \frac{\gamma^+ \gamma_5}{2\sqrt{2}n_r} \psi(z) | \pi \rangle |^Q \Big|_{z^+ = \vec{z}_\perp = 0} \quad (24)$$

The \vec{k}_\perp integration in Eq. (23) is cut off by the ultraviolet cutoff $\Lambda = Q$ implicit in the wavefunction; thus only Fock states with energies $|\mathcal{E}| < Q^2$ contribute.

It is important to note that the distribution amplitude is gauge invariant. In gauges other than light-cone gauge, a path-ordered “string operator” $P \exp(\int_0^1 ds i g A(sz) \cdot z)$ must be included between the $\bar{\psi}$ and ψ . The line integral vanishes in light-cone gauge because $A \cdot z = A^+ z^-/2 = 0$ and so the factor can be omitted in that gauge. This (non-perturbative) definition of ϕ uniquely fixes the definition of T_H which must itself then be gauge invariant.

Is PQCD Factorization Applicable to Exclusive Processes?

One of the concerns in the derivation of the PQCD results for exclusive amplitudes is whether the momentum transfer carried by the exchanged gluons in the hard scattering amplitude T_H is sufficiently large to allow a safe application of perturbation theory.⁴⁴ The problem appears to be especially serious if one assumes a form for the hadron distribution amplitudes $\phi_H(x_i, Q^2)$ which has strong support at the endpoints, as in the QCD sum rule model forms suggested by Chernyak and Zhitnitskii.⁴⁵

This problem has now been clarified by two groups: Gari *et al.*⁴⁶ in the case of baryon form factors, and Mankiewicz and Szczepaniack,⁴⁷ for the case of meson form factors. Each of these authors has pointed out that the assumed non-perturbative input for the distribution amplitudes must vanish strongly in the endpoint region; otherwise, there is a double counting problem for momentum transfers occurring in the hard scattering amplitude and the distribution amplitudes. Once one enforces this constraint, (e.g. by using exponentially suppressed wavefunctions³²) on the basis functions used to represent the QCD moments, or uses a sufficient number of polynomial basis functions, the resulting distribution amplitudes do not allow significant contribution to the high Q^2 form factors to come from soft gluon exchange region. The comparison of the PQCD predictions with experiment thus becomes phenomenologically and analytically consistent. The analysis of exclusive reactions outlined in these lectures based on the effective Lagrangian method is also consistent with this approach. In addition, as discussed by Botts,⁴⁸ potentially soft contributions to large angle hadron-hadron scattering reactions from Landshoff pinch contributions⁴⁹ are strongly suppressed by Sudakov form factor effects.

There also has been important progress testing PQCD experimentally using measurements of the $p \rightarrow N^*$ form factors. In a recent new analysis of existing SLAC data, Stoler⁵⁰ has obtained measurements of several transition form factors of the proton to resonances at $W = 1232, 1535$, and 1680 MeV. As is the case of the elastic proton form factor, the observed behavior of the transition form factors to the $N^*(1535)$ and $N^*(1680)$ are each consistent with the Q^{-4} fall-off and dipole scaling predicted by PQCD and hadron helicity conservation over the measured range $1 < Q^2 < 21$ GeV 2 . In contrast, the $p \rightarrow \Delta(1232)$ form factor

decreases faster than $1/Q^4$ suggesting that non-leading processes are dominant in this case. Remarkably, this pattern of scaling behavior is what is expected from PQCD and the QCD sum rule analyses,⁴⁵ since, unlike the case of the proton and its other resonances, the distribution amplitude $\phi_{N^*}(x_1, x_2, x_3, Q)$ of the Δ is predicted to be nearly symmetric in the x_i , and as first discussed by Carlson and Poor⁵¹ a symmetric distribution leads to a strong cancellation of the leading helicity-conserving terms in the matrix elements of the hard scattering amplitude for $qqq \rightarrow \gamma^* qqq$. These successes of the PQCD approach, together with the evidence for color transparency in quasi-elastic pp scattering gives strong support for the validity of PQCD factorization for exclusive processes at moderate momentum transfer. It seems difficult to understand this pattern of form factor behavior if it is due to simple convolutions of soft wavefunctions.

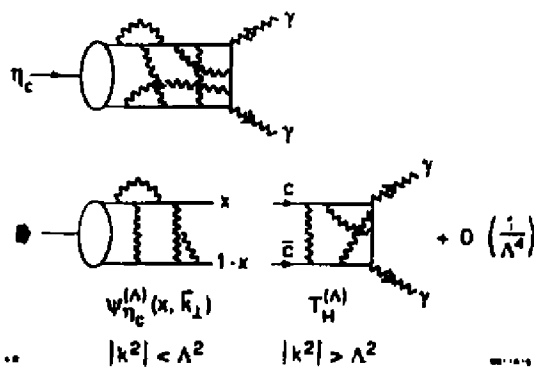


Figure 9: Factorization of perturbative and non-perturbative contributions to the decay $\eta_c \rightarrow \gamma\gamma$. The matrix element $T_H(c\bar{c} \rightarrow \gamma\gamma)$ is calculated from the heavy quark effective Lagrangian with $\Lambda^2 \sim m_Q^2$.

LIGHT-CONE QUANTIZATION AND HEAVY PARTICLE DECAYS

We can now apply the PQCD formalism outlined above for large momentum transfer exclusive processes to heavy quark decays. For example for the decay $\eta_c \rightarrow \gamma\gamma$ we can choose the Lagrangian cutoff $\Lambda^2 \sim m_c^2$. To leading order in $1/m_c$, all of the bound state physics and virtual loop corrections are contained in the $c\bar{c}$ Fock wavefunction $\psi_{\eta_c}(x_i, k_{\perp i})$. The hard scattering matrix element of

the effective Lagrangian coupling $c\bar{c} \rightarrow \gamma\gamma$ contains all of the higher corrections in $\alpha_s(\Lambda^2)$ from virtual momenta $|k^2| > \Lambda^2$. Thus

$$\begin{aligned} \mathcal{M}(\eta_c \rightarrow \gamma\gamma) &= \int d^2 k_\perp \int_0^1 dx \psi_{\eta_c}^{(\Lambda)}(x, k_\perp) T_H^{(\Lambda)}(c\bar{c} \rightarrow \gamma\gamma) \\ &\Rightarrow \int_0^1 dx \phi(x, \Lambda) T_H^{(\Lambda)}(c\bar{c} \rightarrow \gamma\gamma) \end{aligned} \quad (25)$$

where $\phi(x, \Lambda^2)$ is the η_c distribution amplitude. This factorization and separation of scales is shown in Fig. 9. Since the η_c is quite non-relativistic, its distribution amplitude is peaked at $x = 1/2$ and its essentially equivalent to the wavefunction at the origin $\psi(\vec{r} = \vec{0})$.

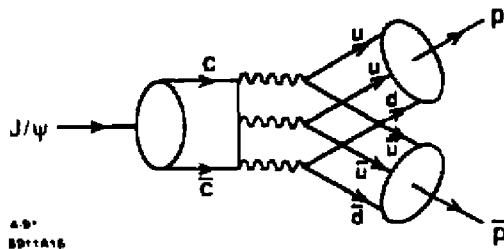


Figure 10 Calculation of $J/\psi \rightarrow p\bar{p}$ in PQCD.

One of the most interesting examples of quarkonium decay in PQCD is the annihilation of the J/ψ into baryon pairs. The calculation involves the convolution of the hard annihilation amplitude $T_H(c\bar{c} \rightarrow ggg \rightarrow uuduud)$ with the J/ψ , baryon, and anti-baryon distribution amplitudes.^{20,45} (See Fig. 10.) The magnitude of the computed decay amplitude for $\psi \rightarrow \bar{p}p$ is consistent with experiment assuming the proton distribution amplitude computed from QCD sum rules.⁴⁵ The angular distribution of the proton in $e^+e^- \rightarrow J/\psi \rightarrow p\bar{p}$ is consistent with hadron helicity conservation; i.e. opposite proton and anti-proton helicity.

The effective Lagrangian method has been used by Lepage, Caswell, and Thacker¹⁰ to systematically compute the order $\alpha_s(\hat{Q})$ corrections to the hadronic

and photon decays of quarkonium. The scale \hat{Q} can then be set by incorporating vacuum polarization corrections into the running coupling constant.¹⁷ A complete summary of the results can be found in Ref. 52.

Annihilation of Quarkonium to Exclusive Channels

One of the outstanding puzzles in charmonium physics is why the J/ψ decays with a large branching ratio into vector plus pseudoscalar mesons: $BR(J/\psi \rightarrow \rho\pi) = (1.28 \pm 0.10) \times 10^{-2}$, and $BR(J/\psi \rightarrow K^*\bar{K}) = (3.8 \pm 0.7) \times 10^{-3}$, whereas $BR(\psi' \rightarrow \rho\pi) < 8.3 \times 10^{-5}$, and $BR(\psi' \rightarrow K^*\bar{K}) < 1.79 \times 10^{-5}$. PQCD predicts a strong suppression into such channels since they necessarily violate hadron helicity conservation.³⁶ The ψ' appears to respect this theorem. However, the pseudo-scalar vector decays of the J/ψ are highly anomalous if they arise from short-distance decay subprocesses in QCD.

The puzzle would be solved⁵³ if there exists a $J^{PC} = 1^{--}$ gluonium state with mass sufficiently close to the J/ψ (but not to the ψ') to affect its hadronic decays.

However, that is not the only puzzle. The branching ratios for the decay of the η_c into two vector mesons ($\rho\rho, K^*\bar{K}^*, \phi\phi$) and also $p\bar{p}$ are not small even though they are all first-order forbidden by hadron helicity conservation in PQCD. However, as pointed out by Anselmino, Genovese, and Predazzi,⁵⁴ these decays would be affected by the presence of a tri-gluonium pseudoscalar state with a mass close (within 60 MeV) to the η_c . It is in fact plausible that a 1^{--} gluonium state is found near the J/ψ , that a 0^{++} gluonium state will also be found near the η_c . The test of this explanation is that the more massive quarkonium states obey the hadron helicity conservation selection rules.

Exclusive Weak Decays of Heavy Hadrons

An important application of the PQCD effective Lagrangian formalism is to the exclusive decays of heavy hadrons to light hadrons, such as $B^0 \rightarrow \pi^+\pi^-$, K^+, K^- .²¹ To a good approximation, the decay amplitude $\mathcal{M} = \langle B|H_{Wk}|\pi^+\pi^-\rangle$ is caused by the transition $\bar{b} \rightarrow W^+\bar{u}$; thus

$$\mathcal{M} = f_\pi p_\pi^\mu G_F / \sqrt{2} \langle \pi^- | J_\mu | B^0 \rangle \quad (26)$$

where J_μ is the $\bar{b} \rightarrow \bar{u}$ weak current. The problem is then to recouple the spectator d quark and the other gluon and possible quark pairs in each B^0 Fock state to the corresponding Fock state of the final state π^- . (See Fig. 11.) The kinematic constraint that $(p_B - p_\pi)^2 = m_\pi^2$ then demands that at least one quark line is far off shell: $p_\pi^2 = (y p_B - p_\pi)^2 \sim -\mu m_B \sim -1.5 \text{ GeV}^2$, where we have noted that the light quark takes only a fraction $(1-y) \sim \sqrt{(k_\perp^2 + m_d^2)/m_B}$ of the heavy meson's momentum since all of the valence quarks must have nearly equal velocity in a bound state. In view of the successful applications⁵⁰ of PQCD factorization to form factors at momentum transfers in the few GeV^2 range, it is reasonable to assume that $\langle |p_\pi^2| \rangle$ is sufficiently large compared to $\Lambda_{\overline{MS}}^2$ that we can begin to apply perturbative QCD methods.

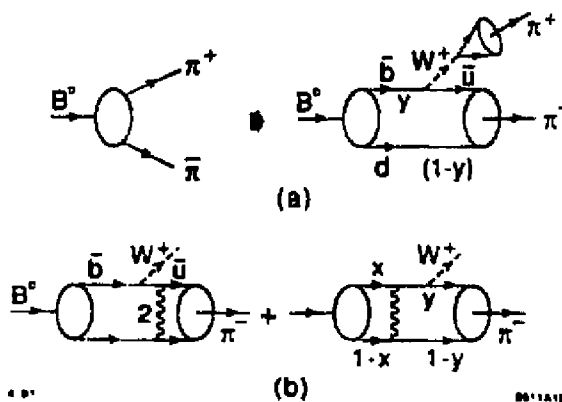


Figure 11: Calculation of the weak decay $B \rightarrow \pi\pi$ in the PQCD formalism of Ref. 21. The gluon exchange kernel of the hadron wavefunction is exposed where hard momentum transfer is required.

The analysis of the exclusive weak decay amplitude can now be carried out in parallel to the PQCD analysis of electroweak form factors⁵⁵ at large Q^2 . The first step is to iterate the wavefunction equations of motion so that the large momentum transfer through the gluon exchange potential is exposed. The heavy quark decay amplitude can then be written as a convolution of the hard scattering amplitude for $Q\bar{q} \rightarrow W^+ \bar{q}\bar{q}$ convoluted with the B and π distribution amplitudes. The minimum number valence Fock state of each hadron gives the leading power law contribution. Equivalently, we can choose the cut-off scale in the effective

Lagrangian $\Lambda^2 < \mu m_B$ so that the hard scattering amplitude $T_H(Q\bar{q} \rightarrow W^+ q\bar{q})$ must be computed from the matrix elements of the order $1/\Lambda^2$ terms in $\delta\mathcal{L}$. Thus T_H contains all perturbative virtual loop corrections of order $\alpha_s(\Lambda^2)$. The result is the factorized form:

$$\mathcal{M}(B \rightarrow \pi\pi) = \int_0^1 dx \int_0^1 dy \phi_B(y, \Lambda) T_H \phi_\pi(x, \Lambda) \quad (27)$$

which is rigorously correct up to terms of order $1/\Lambda^4$. All of the non-perturbative corrections with momenta $|k^2| < \Lambda^2$ are summed in the distribution amplitudes.

In order to make an estimate of the size of the $B \rightarrow \pi\pi$ amplitude we shall take the simplest possible forms for the required wavefunctions

$$\phi_\pi(y) \propto \gamma_5 \not{p}_\pi y(1-y) \quad (28)$$

for the pion and

$$\phi_B(x) \propto \frac{\gamma_5 [\not{p}_B + m_B g(x)]}{\left[1 - \frac{1}{x} - \frac{\epsilon^2}{(1-x)}\right]^2} \quad (29)$$

for the B, each normalized to its meson decay constant. The above form for the heavy quark distribution amplitude is chosen so that the wavefunction peaks at equal velocity; this is consistent with the phenomenological forms used to describe heavy quark fragmentation into heavy hadrons. We estimate $\epsilon \sim 0.05$ to 0.10. The functional dependence of the mass term $g(x)$ is unknown; however, it should be reasonable to take $g(x) \sim 1$ which is correct in the weak binding approximation.

One now can compute the leading order PQCD decay amplitude

$$\mathcal{M}(B^0 \rightarrow \pi^+ \pi^-) = \frac{G_F}{\sqrt{2}} V_{ud}^* V_{ub} P_{\pi^+}^\mu \langle \pi^- | V^\mu | B^0 \rangle \quad (30)$$

where

$$\begin{aligned}
 \langle \pi^- | V^\mu | B^0 \rangle &= \frac{8\pi\alpha_s(Q^2)}{3} \int_0^1 dx \int_0^{1-x} dy \phi_B(x) \phi_\pi(y) \\
 &\times \frac{\text{Tr}[\not{p}_{\pi^-} \gamma_5 \gamma^\mu \not{k}_1 \gamma^\nu (\not{p}_B + M_B g(x)) \gamma_5 \gamma_\nu]}{k_1^2 Q^2} \\
 &+ \frac{\text{Tr}[\not{p}_{\pi^-} \gamma_5 \gamma^\nu (\not{k}_2 + M_B) \gamma^\mu (\not{p}_B + M_B g(x)) \gamma_5 \gamma_\nu]}{(k_2^2 - M_B^2) Q^2}
 \end{aligned} \tag{31}$$

Numerically, this gives the branching ratio

$$BR(B^0 \rightarrow \pi^+ \pi^-) \sim 10^{-8} \xi^2 N \tag{32}$$

where $\xi = 10|V_{ub}/V_{cb}|$ is probably less than unity, and N has strong dependence on the value of g : $N = 180$ for $g = 1$ and $N = 5.8$ for $g = 1/2$. The present experimental limit⁵⁶ is

$$BR(B^0 \rightarrow \pi^+ \pi^-) < 3 \times 10^{-4}. \tag{33}$$

A similar PQCD analysis can be applied to other two-body decays of the B : the ratios of the widths will not be so sensitive to the form of the distribution amplitude, allowing tests of the flavor symmetries of the weak interaction.

LEADING TWIST QCD PREDICTIONS FOR HEAVY QUARK PRODUCTION

We now turn to one of the most important applications of QCD to collider physics – the production of heavy quarks.⁵⁷ It is well known that the dominant QCD contributions to heavy quark production in hadronic collisions is computed from the sum of leading twist gg and $q\bar{q}$ fusion subprocess cross sections.⁵⁸ The

resulting hadronic cross section obeys QCD factorization:

$$\frac{d\sigma(H_A H_B \rightarrow Q\bar{Q})}{d^3 p/E} = \sum_i \times \int dx_1 dx_2 \frac{d\sigma_{i,j}(x_1 P_A, x_2 P_B, \alpha_s(\hat{Q}^2))}{d^3 p/E} G_i(x_1, \hat{Q}_1) G_j(x_2, \hat{Q}_2) . \quad (34)$$

It seems remarkable that the same structure functions that appear here also appear in deep inelastic lepton scattering even in the case of heavy ion collisions, since intuitively one would expect strong initial state distortions of the nuclear structure functions. In fact such initial state interactions will not affect the inclusive cross section if the target length conditions $E_a > \mu^2 L_B$ and $E_b > \mu^2 L_A$ are satisfied, where E_a is the energy of parton a in the rest frame of target B and μ^2 is a characteristic QCD mass scale.⁵⁹ At such high energies, coherence occurs between Glauber scattering on different target centers, and there is insufficient time for the parton to have an inelastic reaction which can change its mass by as much as μ^2 . Below this scale, normal attenuation occurs. However initial state interactions will always lead to an excess of central region multiplicity and an increase of the heavy quark pair transverse momentum. However, if the target length conditions are satisfied, this is a unitary effect which does not effect the total integrated heavy quark production rate. Proofs that this factorization is valid to all orders in perturbation theory to leading order in $1/m_Q^2$ have been outlined by Collins, Soper, and Sterman,⁶⁰ and by Bodwin,⁶¹ A recent analysis by Qiu and Sterman⁶² shows that the factorization of structure functions and subprocess cross sections is even valid to next to leading order in $1/m_Q^2$.

The calculation of the next to leading order in $\alpha_s(\hat{Q}^2)$ corrections to this result is highly non-trivial. The main results are given in Refs. 63 and 64. An essential point is that very large corrections from $2 \rightarrow 3$ subprocesses cross sections such as $gg \rightarrow Q\bar{Q}g$ contribute to this order reflecting the importance of having a spin-one gluon in the t -channel. In fact the gluon exchange subprocesses actually dominate the leading order $2 \rightarrow 2$ annihilation subprocesses in the forward direction and at $x_1 x_2 s \gg m_Q^2$.

I have indicated in the QCD factorized formula that three high momentum scales must be determined: the value of \hat{Q} in the perturbative expansion of the

subprocess cross section and the values of \hat{Q}_1, \hat{Q}_2 which set the QCD evolution scale of each structure function. However, it is not universally agreed on how or even whether one should try to set these scales in the lowest order predictions. In my view there is no such ambiguity: Lepage, Mackenzie, and I¹⁷ have advocated a procedure called "automatic scale fixing." Once one chooses a definite renormalization scheme to define and normalize the running coupling constant, one can set each scale \hat{Q} by requiring that the form of the predictions has no explicit dependence on the number of light fermion pairs: i.e. that the effects of fermion pair factorization are all correctly summed in the running coupling constant. This procedure is equivalent to the standard procedure used in QED.

In addition to these leading twist contributions to heavy quark production, we will also need to consider higher twist (power-law suppressed in $1/m_Q^2$) contributions which arise from the heavy quark content of the hadron wavefunctions themselves. The analysis and effect of such components is discussed in the next sections.

THE HEAVY QUARK CONTENT OF NUCLEONS

One of the most intriguing unknowns in nucleon structure is the strange and charm quark structure of the nucleon wavefunction.⁶⁵ The EMC spin crisis measurements indicate a significant $s\bar{s}$ content of the proton, with the strange quark spin strongly anti-correlated with the proton spin. Just as striking, the EMC measurements⁶⁶ of the charm structure function of the Fe nucleus at large $x_b \sim 0.4$ appear to be considerably larger than that predicted by the conventional photon-gluon fusion model, indicating an anomalous charm content of the nucleon at large values of x . The probability of intrinsic charm has been estimated⁶⁶ to be 0.3%.

As emphasized in the previous sections, the physical content of a hadron in terms of its quark and gluon constituents can be represented by its light-cone wavefunctions $\psi_n(x_i, p_{\perp i}, \lambda_i)$, which are given by the projection of the hadron wavefunction on the complete set of Fock states defined at fixed light-cone time $\tau = t + z/c$.³² Here $x_i = (E_i + p_{Li})/(E + p_L)$, with $\sum_i x_i = 1$, is the fractional (light-cone) momentum carried by parton i . The determination of the light-cone

wavefunctions requires diagonalizing the light-cone Hamiltonian on the free Fock basis. This in fact has been done for QCD in one-space and one time dimension using a momentum space method of discretization called discretized light-cone quantization (DLCQ).³⁹ Efforts are now proceeding to solve the much more complex problem in 3+1 dimensions. Even without explicit solutions, a great deal of information can be obtained at high k_\perp or the end-point $x \sim 1$ region using perturbative QCD since the quark and gluon propagators become far off-shell. In particular one can obtain dimensional and spectator counting rules which determine the end-point behavior of structure functions, etc.

One of the most successful applications of the DLCQ method has been to QCD in one-space and one time dimensions. Complete numerical solutions have been obtained for the meson and baryon spectra as well as their respective light cone Fock state wavefunctions for general values of the coupling constant, quark masses, and color.

In Fig. 12 I show recent results obtained by Hornbostel⁶⁷ for the structure functions of the lowest mass meson in QCD(1+1) wavefunctions for $N_c = 3$ and two quark flavors. As seen in the figure, the heavy quark distribution arising from the $q\bar{q}Q\bar{Q}$ Fock component has a two-hump character. The second maximum is expected since the constituents in a bound state tend to have equal velocities. The result is insensitive to the value of the Q^2 of the deep inelastic probe. Thus intrinsic charm is a feature of exact solutions to QCD(1+1). Note that the integrated probability for the Fock states containing heavy quarks falls nominally as g^2/m_Q^4 in this super-renormalizable theory, compared to g^2/m_Q^2 dependence expected in renormalizable theories.

In the case of QCD(3+1), we also expect a two component structure for heavy quark structure functions of the light hadrons. The low x_F enhancement reflects the fact that the gluon-splitting matrix elements of heavy quark production favor low x . On the other hand, the $Q\bar{Q}q\bar{q}$ wavefunction also favors equal velocity of the constituents in order to minimize the off-shell light-cone energy and the invariant mass of the Fock state constituents. In addition, the non-Abelian effective Lagrangian analysis discussed above allows a heavy quark fluctuation in the bound state wavefunction to draw momentum from all of the hadron's valence quarks

at order $1/m_Q^2$. This implies a significant contribution to heavy quark structure functions at medium to large momentum fraction x . The EMC measurements of the charm structure function of the nucleon appear to support this picture.⁶⁶

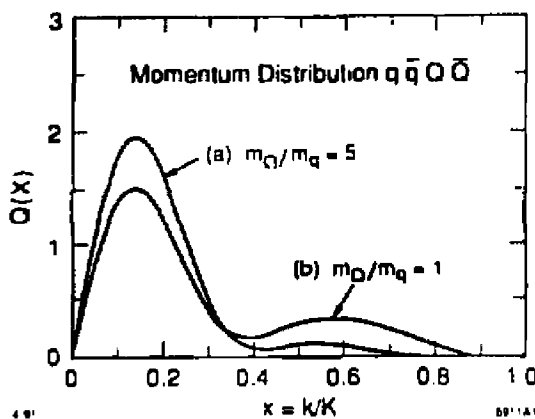


Figure 12 The heavy quark structure function $Q(x) = Gq/M(x)$ of the lightest meson in QCD(1+1) with $N_c = 3$ and $g/m_q = 10$. Two flavors are assumed with (a) $m_Q/m_q = 1.001$ and (b) $m_Q/m_q = 5$. The curves are normalized to unit area. The probability of the $q\bar{q}Q\bar{Q}$ state is 0.56×10^{-2} and 0.11×10^{-4} , respectively. The DLCQ method for diagonalizing the light-cone Hamiltonian is used with anti-periodic boundary conditions. The harmonic resolution is taken at $K = 10/2$. (From Ref. 67.)

It is thus useful to distinguish *extrinsic* and *intrinsic* contributions to structure functions. The extrinsic contributions are associated with the substructure of a single quark and gluon of the hadron. Such contributions lead to the logarithmic evolution of the structure functions and depend on the momentum transfer scale of the probe. The intrinsic contributions involve at least two constituents and are associated with the bound state dynamics independent of the probe. (See Fig. 13.) The intrinsic gluon distributions are closely related to the retarded mass-dependent part of the bound-state potential of the valence quarks. A rather complete model for the intrinsic gluon distribution of the proton including helicity correlations that satisfies known constraints is given in Ref. 68.

It is also important to distinguish extrinsic and intrinsic contributions to the sea quark distributions. For example, the extrinsic contributions to the charm quark sea only depends logarithmically on the charm quark mass at $Q^2 \gg m_c^2$. The intrinsic contributions are suppressed by two or more inverse powers of the

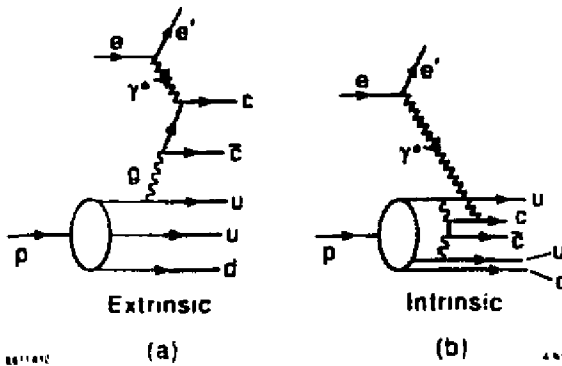


Figure 13. Illustrations of (a) extrinsic (leading twist) and (b) intrinsic (higher twist $O(\mu^2/m_c^2)$) QCQ contributions to the charm structure function of the proton $G_{c/p}(x)$. The magnitude of the intrinsic contribution is controlled by the multi-gluon correlation parameter μ in the proton wavefunction. The intrinsic contribution dominates $G_{c/p}(x)$ at large x .

heavy quark mass. Nevertheless, these contributions can still be important and dominate in certain kinematic regions, particularly large x . The intrinsic contributions have a number of remarkable properties which we return to below.

It is well-known that the light-cone Fock state expansion is physically equivalent to the ordinary equal time description of a hadron moving at large momentum P . For example, to describe $e p$ scattering in the CM or HERA colliding beam configuration we consider the equal time Fock expansion of the proton in QCD,

$$|p\rangle = |uud\rangle + |uudq\rangle + \dots + |uudQ\bar{Q}\rangle + \dots \quad (35)$$

where $q(Q)$ refers to a light (heavy) quark and g to a gluon. At high energies, most scattering processes in electroproduction only involve states of the proton that were formed long before the collision takes place. The individual Fock components "lifetimes" Δt (before mixing with other components) which can be estimated from the uncertainty relation $\Delta E \Delta t \sim 1$. At large hadron energies E the energy difference becomes small.

$$\Delta E \approx \frac{1}{2E} \left(m^2 - \sum_i \frac{m_i^2 + p_{Ti}^2}{x_i} \right). \quad (36)$$

Fock components for which $1/\Delta E$ is larger than the interaction time have thus formed before the scattering and can be regarded as independent constituents

of the incoming wavefunction. At high energies only collisions with momentum transfers commensurate with the center of mass energy, such as deep inelastic lepton scattering ($Q^2 \sim 2mv$) and jet production with $p_T \sim \mathcal{O}(E_{cm})$ produce states with lifetimes as short as the scattering time.

The above arguments show that a typical scattering process is essentially determined by the mixture of incoming Fock states, i.e. by the wavefunctions of the scattering particles. This is true even for collisions with very heavy quarks or with particles having very large p_T in the final state, provided only that the momentum transferred in the collision is small compared to E_{cm} . The cross sections for such collisions are thus determined by the probability of finding the corresponding Fock states in the beam or target particle wavefunctions; cf. Eq. (35). An example of this is provided by the Bethe-Heitler process of e^+e^- pair production in QED. A high energy photon can materialize in the Coulomb field of a nucleus into an e^+e^- pair through the exchange of a very soft photon. The creation of the massive e^+e^- pair occurs long before the collision and is associated with the wave function of the photon. The collision process itself is soft and does not significantly change the momentum distribution of the pair. Similarly, heavy quark production in hadron collisions or electroproduction at any Q^2 at high energies ($E_{cm} \gg m_Q$) is governed by the hard (far off energy-shell) components of the hadronic wavefunction.

THE STRUCTURE OF INTRINSICALLY-HARD STATES¹⁶

The leading extrinsic contribution to is one gluon splitting into a heavy quark pair, $G \rightarrow Q\bar{Q}$ (Fig. 13(a)). We call this contribution extrinsic since it is independent of the hadron wavefunction, except for its gluon content. The extrinsic heavy quarks are, in a sense, "constituents of the gluon". The extrinsic heavy quark wave function has the form

$$\Psi^{\text{extrinsic}}(q\bar{q}Q\bar{Q}) = \Gamma_G T_H(G \rightarrow Q\bar{Q}) \frac{1}{E \Delta E}. \quad (37)$$

The square of the gluon amplitude Γ_G gives the ordinary gluon structure function of the hadron. The gluon splitting amplitude T_H is of order $\sqrt{\alpha_s(m_Q^2 + p_T^2 Q)}$.

and ΔE is the energy difference (36). The integral of the extrinsic probability $|\Psi^{\text{extrinsic}}|^2$ over p_{TQ}^2 for $p_{TQ} \lesssim \mathcal{O}(m_Q)$ brings a factor of m_Q^2 . Hence we see that the probability of finding extrinsic heavy quarks (or large p_T) in a hadronic wavefunction is only logarithmically dependent on the quark mass (or p_T). The production cross section of the $Q\bar{Q}$ pair is still damped by a factor $1/m_Q^2$, this being the approximate transverse area of the pair.

Intrinsic heavy quark Fock states¹³ arise from the spatial overlap of light partons. A typical diagrams is shown in Fig. 13(b). The transverse distance between the participating light partons must be $\lesssim \mathcal{O}(1/m_Q)$ for them to be able to produce the heavy quarks. The wave function of the intrinsic Fock state has the general structure

$$\Psi^{\text{intrinsic}}(q\bar{q}Q\bar{Q}) = \Gamma_{ij} T_H(ij \rightarrow Q\bar{Q}) \frac{1}{E\Delta E}. \quad (38)$$

Here Γ_{ij} is the two-parton wavefunction, which has a dimension given by the inverse hadron radius. $T_H(ij \rightarrow Q\bar{Q})$ is the amplitude for two (or, more generally, several) light partons i,j to create the heavy quarks, and ΔE is the energy difference (36) between the heavy quark Fock state and the hadron. A sum over different processes, and over the momenta of the light partons, is implied in (38). In renormalizable theories such as QCD, the amplitude T_H is dimensionless. Hence, up to logarithms, the probability $|\Psi^{\text{intrinsic}}|^2$ for intrinsic heavy quarks is of $\mathcal{O}(1/m_Q^2)$ (after the p_T^2 integration). This is smaller by $1/m_Q^2$ as compared to the probability (37) for extrinsic heavy quarks,^{13,69} as is true of higher twist. The relative suppression is due to the requirement that the two light partons be at a distance $\lesssim 1/m_Q$ of each other in the intrinsic contribution. It is easy to see that the intrinsic contributions of a given order in the inverse quark mass correspond to the matrix elements of the heavy quark effective Lagrangian.

In contrast to the extrinsic contribution (3), which depends only on the inclusive single gluon distribution, an evaluation of the intrinsic Fock state (4) requires a knowledge of multiparton distributions amplitudes. In particular, we need also the distribution in transverse distance between the partons. Our relative ignorance of the multiparton amplitudes Γ_{ij} for hadrons makes it difficult to reliably calculate the magnitude of the intrinsic heavy quark probability. We can, however, estimate¹³ the distribution of intrinsic quarks from the size of the energy

denominator ΔE , as given by (36). It is clear that those Fock states which minimize ΔE , and hence have the longest lifetimes, also have the largest probabilities. In fact, taking

$$|\Psi^{\text{intrinsic}}|^2 \sim 1/(\Delta E)^2, \quad (39)$$

one finds that the maximum is reached for

$$x_t = \frac{\sqrt{m_i^2 + p_{T,i}^2}}{\sum_i \sqrt{m_i^2 + p_{T,i}^2}}, \quad (40)$$

implying equal (longitudinal) velocities for all partons. The rule (39) has been found to successfully describe the hadronization of heavy quarks.^{70,71}

Using the probability (39), we see from (40) that partons with the largest mass or transverse momentum carry most of the longitudinal momentum. This has long been one of the hallmarks of intrinsic charm. We also note that the intrinsic heavy quark states have a larger transverse size than the extrinsic ones, although both tend to be small, of $\mathcal{O}(1/m_Q^2)$. The extrinsic heavy quarks are produced by a single (pointlike) gluon, (Fig. 14(a)) whereas the intrinsic mechanism is more peripheral (Fig. 14(b)). This means that rescattering and absorption effects for intrinsic states produced on heavy nuclei will be relatively more significant, compared to that for extrinsic states. In addition to the heavy quarks Q , such rescattering may affect the light partons involved in the intrinsic state. These light quarks tend to be separated by a larger transverse distance than the heavy quarks, further enhancing the rescattering.

Consider now the formation of intrinsic heavy quark states in nuclear wave functions. At high energies, partons from different nucleons can overlap, provided only that their transverse separation is small. Thus the partons which create intrinsic heavy quarks can come from two nucleons which are separated by a longitudinal distance in the nucleus. It is reasonable to assume that partons belonging to different nucleons are uncorrelated, i.e. that the two-parton amplitude Γ_{ij} in Eq. (38) is proportional to the product $\Gamma_i \Gamma_j$ of single parton amplitudes. Hence the amount of intrinsic charm in nuclei may possibly be more reliably calculated than for hadrons. The probability for intrinsic charm will increase with

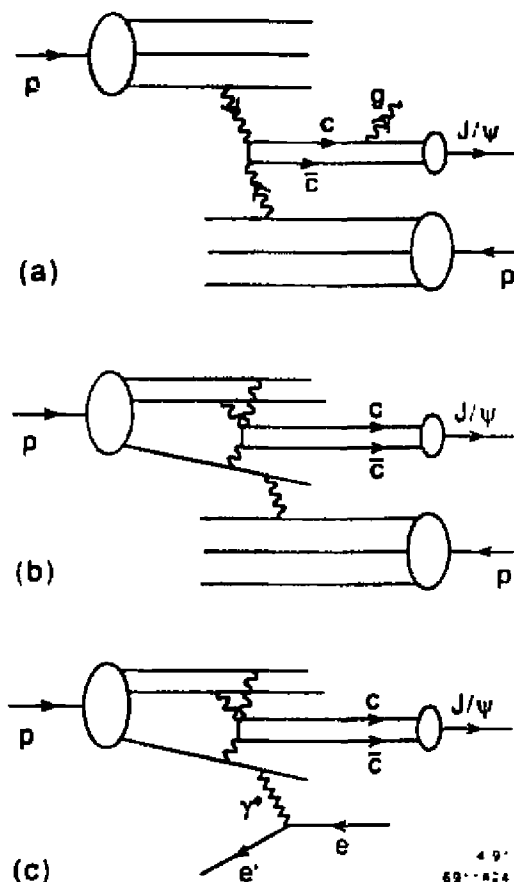


Figure 14 QCD mechanisms for charmonium production (a) Conventional gluon-gluon fusion mechanism (b) Illustration of intrinsic charm contribution to $pp \rightarrow J/\psi X$ due to the "dissipative" excitation of the intrinsic heavy quark Fock state. Notice that the interaction is with a peripheral light quark of the projectile. (c) Illustration of intrinsic charm contribution to $ep \rightarrow e^+ J/\psi X$ due to the "Coulomb" excitation of the intrinsic heavy quark Fock state. Notice that the interaction of the soft photon is with a peripheral light quark of the projectile.

the nuclear path length as $A^{1/3}$. Moreover, the total longitudinal momentum of the intrinsic quark pair, being supplied by two different nucleons, can be larger than in a single hadron, and can in fact exceed the total momentum carried by one nucleon.

All that we have said above concerning heavy quark Fock states applies equally to states with light partons carrying large transverse momentum. Using Eq. (39) as a guideline for the probability of intrinsic hardness, we see in

fact that the parton mass and p_T appear in an equivalent way. Remarkably, QCD predicts that these high mass fluctuations occur in the nucleon and nuclear wavefunctions with the minimal power law fall off: $P(M^2 > M_0^2) \sim 1/M_0^2$. We again expect that the intrinsic mechanism will be dominant at large x_F , and in particular in the cumulative ($x_F > 1$) region of nuclear wavefunctions. In each case one can materialize the large mass fluctuations in electroproduction even at minimal photon mass Q^2 . The crucial experimental requirement is the ability to identify the target fragments in the target fragmentation region.

CONSEQUENCES OF INTRINSIC HEAVY QUARKS IN HADRONIC AND NUCLEAR COLLISIONS¹⁶

The concept of intrinsic charm was originally inspired by hadron-hadron scattering experiments⁷² showing unexpectedly abundant charm production at large $x_F = 2p_{\text{charm}}/E_{\text{cm}}$. When extrapolated to small x_F , the data suggested total charm cross sections in the millibarn range, far beyond the predictions (20 - 50 μb) of the standard QCD gluon fusion process, illustrated in Fig. 14(a). Later data with good acceptance at low x_F showed that the total charm cross section actually is compatible with the gluon fusion process.⁷³ Nevertheless, more evidence was also obtained showing that charm production at large x_F , albeit a small fraction of the total cross section, remains larger than expected.⁷⁴ The large x_F data also shows correlations (leading particle effects) with the quantum numbers of the beam hadron that are incompatible with gluon fusion.⁷⁵

The intrinsic charm production mechanism (Fig. 14(b)) would normally be expected to give a contribution smaller than the extrinsic one, due to the $1/m_Q^2$ suppression from the requirement of spatial overlap of initial light partons. However, at sufficiently large x_F the intrinsic mechanism will dominate, because the momentum of several incoming partons can be transferred to the heavy quarks.

Experiments on charm production from nuclear targets have also shown an anomalous dependence on the nuclear number A . If the open charm (D, Λ_c) cross section is parametrized as

$$\frac{d\sigma}{dx_F} \propto A^{\alpha(x_F)} \quad (41)$$

then $\alpha(x_F \sim 0.2) \sim 0.7 \dots 0.9$ is obtained.^{73,76} For heavy nuclei ($A \approx 200$) this means a factor of 2...3 suppression in the cross section, compared to the leading QCD expectation ($\alpha = 1$). In this respect, the charm production data is quite different from that of massive μ -pair production, for which α is found to be very close to 1.⁷⁷

In the following sections I shall argue that intrinsic heavy quarks of the hadronic Fock state wavefunctions allows one to understand the observed deviations from the perturbative QCD predictions based solely on fusion subprocesses. There are, in fact, a number of interesting phenomenological consequences of intrinsic charm and beauty in the proton wavefunction:

- The charm and beauty structure functions of the proton are expected to be much harder than that predicted by photon-gluon fusion. The EMC measurements of the charm structure function measured in $\mu F t \rightarrow \mu \mu X$ has a magnitude approximately 20 times larger than that predicted by fusion. It will be particularly interesting to see if HERA measurements confirm this anomaly and also find a significant b-quark distribution at large x_b .
- Heavy quarkonium can be produced at large x_F in the beam and target fragmentation regions. A dramatic example is low Q^2 Coulomb excitation of the proton in electroproduction $\epsilon p \rightarrow \epsilon' J/\psi X$ where the intrinsic $c\bar{c}$ in the proton can combine their momenta to produce heavy quarkonium states out to large x_F in the proton fragmentation region. (See Fig. 14(c).) This test will be particularly interesting at the HERA ϵp collider, requiring forward acceptance of di-leptons. In this process, the photon excites the proton by interacting with the valence quarks. Hoyer, Mueller, and I¹⁴ have estimated that intrinsic hardness leads to cross sections of order

$$\frac{d\sigma}{d \log Q^2} \sim \frac{(1 - x_F)^2}{M_{Q\bar{Q}}^4},$$

and

$$\frac{d\sigma}{d \log \bar{Q}^2} \sim \frac{(1 - x_F)^2}{M_{Q\bar{Q}}^6}, \quad (42)$$

The normalization and mass scale of these terms is supplied by the multi-

particle distribution amplitudes in the proton wavefunction.

- More generally, soft gluon exchange with spectator quarks in intrinsic heavy quark Fock states can lead to significant cross sections for charmonium and upsilon production at large x_F in hadronic collisions. In fact, as we shall emphasize in later sections there is ample evidence for anomalously large J/ψ production in proton and pion induced reactions. In fact the NA3 experiment has even observed the coincident production of two J/ψ particles with total $x_F > 0.8$.
- Charm and beauty baryons and mesons can be produced at large x_F by the recombination of the intrinsic heavy quark with co-moving spectators in the hadronic wavefunction. Again, the soft gluon or Pomeron interaction with the target can be with the peripheral spectators of the beam hadron,¹⁴ not necessarily the heavy quark pair. This mechanism can account for the observations of high x_F Λ_c ($dN/dx_F \sim (1 - x_F)^2$) seen in several ISR experiments,⁷⁸ the high x_F $\Xi(\text{csu})$ state observed in the hyperon beam experiment WA62⁷⁴ ($dN/dx_F \sim (1 - x_F)^{1/7}$), the high x_F excess of D and \bar{D} mesons reported by the LEBC-EHS experiment in $p\bar{p}$ collisions, and the anomalous charm production results of the $n\bar{A}$ experiment E400. Intrinsic heavy quarks imply that the distribution of charm and beauty hadrons at low transverse momentum will be much more copious at large rapidities at the SSC and LHC than usually assumed.
- The fact that the production of the intrinsic charm system can be accomplished by collisions of the peripheral quarks at relatively large impact distances in the incident Fock state implies that the main interaction in a nuclear target tends to occur on the front surface of the nucleus. This can account for the observations by NA3 and E772 that charmonium production in hadron nucleus collisions is proportional to $A^{0.71 \sim 0.77}$ at large x_F where intrinsic charm dominates over fusion mechanisms.
- The presence of intrinsic charm in the proton implies that charm production at threshold can be considerably larger than expected from fusion mechanisms. This can be tested in exclusive charm electroproduction reactions such as $\gamma^* p \rightarrow \bar{D} \Lambda_c$, cross sections near threshold. Such measurements of

constrained charmed meson and charmed baryon final states can be used to determine charmed baryon decay branching ratios, one of the major uncertainties in the present determinations of the charmed baryon production cross sections in hadron collisions.

- The hardness of the intrinsic heavy quark distributions in the proton implies that the average energy of parton-parton subprocesses initiated by such parton distributions will be higher than gluon-induced reactions.
- The enhanced coupling of Higgs particles to heavy quarks compensates for the power law suppression of the intrinsic heavy quarks. Thus searches for the Higgs based on intrinsic heavy quark distributions at large x_F may be advantageous for high energy pp colliders.

It thus is natural to attribute the anomalous nuclear dependence shown by the charm production data with the dominance of the intrinsic charm component at large x_F . As I review in the next sections, the necessity for intrinsic heavy quark contributions is especially clear in heavy quarkonium production.

SUPPRESSION OF HEAVY QUARKONIUM PRODUCTION IN NUCLEAR COLLISIONS³⁰

One of the most striking nuclear effects in QCD is the observation at CERN by NA-38²⁹ that the ratio of J/ψ production to the lepton pair continuum is strongly suppressed in nucleus-nucleus collisions. The suppression of this ratio increases with the associated hadronic transverse energy E_T and decreases with the transverse momentum P_T of the pair. The NA38 results have raised considerable interest since they appear generally consistent with the hope that a quark-gluon plasma could form in high energy heavy ion collisions and thus screen the normal color forces responsible for binding the $Q\bar{Q}$. Such a "quagma" effect is naturally enhanced in events that have high E_T , since high associated multiplicity implies that the two nuclei have collided with maximum overlap. In addition, one expects that the suppression would be strongest in reactions where the pair has low P_T since geometrically the color-screening in the plasma region can then act over longer distances.

If the "quagma" explanation of quarkonium suppression is correct then this

effect should be specific to heavy nucleus-nucleus collisions. However, recent measurements of J/ψ , ψ' , and Υ production in high energy πA and pA collisions at Fermilab by the E772 collaboration²⁸ show that there is a striking suppression of heavy quarkonium production even in hadron nucleus collisions. These results confirm the earlier measurements of the J/ψ nuclear dependence by NA3 and E672. Perhaps the most remarkable result found by E772 is the observation that Υ production in pA collisions is strongly suppressed at negative x_F , i.e. in the nuclear fragmentation region, but not in the proton fragmentation region.

It is clear that one must resolve the origin of heavy quarkonium suppression in hadron-nucleus collisions before one can make any conclusions about quark-gluon plasma effects in heavy ion collisions. It is evident from the data that there must be other non-additive nuclear effects which also can differentially suppress heavy quarkonium production compared to lepton pair production.

Gluon Shadowing

An obvious candidate for the suppression of heavy quarkonium in nuclear collisions is the shadowing of the gluon distribution in the nucleus $G_{g/A}(x, Q) < AG_g/N(x, Q)$ since the gluon-gluon fusion, $gg \rightarrow Q\bar{Q}$ is expected to be the dominant production subprocess in PQCD. However, as emphasized in Ref. 27 the shadowing of the structure function of the nuclear target predicts that the nuclear suppression of the quarkonium cross section should be a factorized function of the gluon momentum fraction x_2 , $d\sigma/dx_F \propto G_{g/A}(x_2) \propto A^{\alpha(x_2)}$.

In the case of J/ψ production, the data on the x_F -dependence of α is particularly detailed,^{79,28} showing a remarkable decrease from $\alpha = 1$ near $x_F = 0$ to $\alpha = 0.7 \dots 0.8$ at large x_F . The data at different beam energies are very similar, implying that Feynman scaling is valid. Thus the nuclear dependence exhibited by the J/ψ data when compared at different energies is actually a function of $x_F = x_1 - x_2$ rather than x_2 . The nuclear suppression does not factorize into a product of beam and target structure functions, as expected in leading twist. The target dependence thus must be due to a higher twist effect, i.e. one that is of $\mathcal{O}(1/m_Q^2)$, compared to the leading (factorizable) QCD process. Moreover, in the case of Υ production the values of the gluon fraction x_2 are too large to expect much shadowing. Certainly gluon shadowing cannot explain the observed

suppression of $pA \rightarrow TX$ production in the negative x_F region.

Although gluon shadowing by itself cannot explain the observed nuclear suppression of heavy quarkonium, it must occur on general grounds. Hung Jung Lu⁸⁰ and I have shown that the nuclear shadowing (suppression below additivity) of parton distributions at low x_b , reflects the nuclear dependence of the (off-shell) anti-parton nucleus cross section at high energies. This result follows from the crossing behavior of the forward parton-nucleus amplitude as in the Landshoff, Polkinghorne, Short⁸¹ model. We also show that in some cases anti-shadowing (an enhancement above additivity) of structure functions occurs due to coherent Reggeon contributions. In our analysis we expect that the nuclear gluon distribution will be shadowed more at $x_b \rightarrow 0$ than nuclear quark distributions since the gluon has stronger Glauber multiple scattering in the nucleus due to its stronger color charge. It is difficult to predict the possible magnitude of gluon anti-shadowing because of uncertainties in the coupling of Reggeon exchange to the forward gluon-nucleon scattering amplitude. A useful estimate and model for gluon shadowing, including its evolution, has been given by Qiu.⁸²

Final State Absorption of Quarkonium

Another mechanism which can suppress heavy quarkonium production in nuclear targets is final state absorption of the $Q\bar{Q}$ bound state, as expected in the standard Glauber analysis. The photoproduction cross section $\gamma A \rightarrow J/\psi X$ is an ideal process to isolate such effects. However, the data show very weak nuclear dependence. In fact SLAC measurements⁸³ imply that the effective J/ψ -nucleon cross section is less than 4 mb at low energies, $E_{\text{lab}} \sim 20$ GeV. At higher energies, the $c\bar{c}$ quarks do not have time to separate significantly inside the nucleus. Thus the J/ψ forms only after the charm quarks have left the nuclear environment, and the suppression cannot be related to the size of the J/ψ wave function.³¹ This is also supported by the E772 data showing that the nuclear suppression for the $\Psi(2S)$ and the J/ψ is the same.²⁸ Thus, because of color transparency and the finite formation time of the charmonium state, one expects that the effective J/ψ -nucleon cross section is even smaller at higher energies. This is due to the fact that the $c\bar{c}$ state is formed with a transverse size of order of the Compton scale $1/m_Q$, and it stays small over a distance proportional to its energy as it

traverses the nucleus. In contrast, the NA3 and Fermilab E537 data show that the nuclear suppression strongly increases with the momentum of the J/ψ . In addition, we note that the T-nucleon interaction cross section is much less than that of the J/ψ due to the much smaller size of the $b\bar{b}$ bound state. Nevertheless, the E772 data shows significant nuclear suppression for T production.

Thus final state absorption of heavy quarkonium cannot account for any of the major features seen in the nuclear production data. Of course, such effects must be present at some level and need to be included in a complete analysis.

Nuclear Suppression Due to Co-Moving Spectators

In any event in which heavy quarks are produced, there are many other spectator quarks and gluons produced in the central and beam and target fragmentation regions. In the case of nuclear targets or beams, multiple scattering processes can lead to a cascade of such secondary partons. Eventually, the spectator partons hadronize to produce the associated multiplicity.

If a given spectator parton has a similar rapidity as the Q or \bar{Q} , then the cross section for it to interact with the heavy quark can be very large. (See Fig. 15.) In fact, a capture reactions such as $q\bar{b} \rightarrow Bg$ at low relative velocity will deplete the production of the T in favor of open B production. Other capture reactions may include quark interchange processes such as $\pi b \rightarrow Bu$ and $pc \rightarrow \Lambda_c u$. As emphasized in Ref. 31, such reactions can account for many of the observed features of heavy quarkonium suppression in nuclei.

As in the case of the quark-gluon plasma processes, the suppression of heavy quarkonium due to capture reactions with co-moving partons occurs more strongly in high E_T and nuclear reactions since there is a higher density of co-moving spectators. This suppression occurs dominantly at low P_T since again that is where there strong parton interactions at low relative velocity. However, unlike the quagma effect, suppression due to co-movers can occur in any type of hadron-hadron or hadron nucleus collision. Thus, at least qualitatively, co-mover interactions can explain the main features of nuclear suppression, including T suppression at negative x_F in pA collisions and J/ψ suppression in nucleus-nucleus collisions as measured by NA38.

However, co-mover interactions cannot explain all of the features of the J/ψ

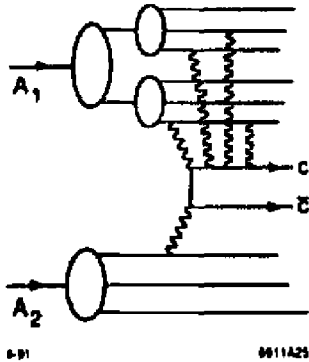


Figure 15. Illustration of the interaction of produced charm quarks with co-moving spectators. The charm quark can coalesce with any co-moving parton created in the nuclear collision, thus enhancing charmed hadron formation at the expense of charmonium production.

nuclear suppression data. In particular, the fact that the suppression of quarkonium production becomes strongest at large values of x_F in hadron-nucleus collisions is not explained, since the density of co-moving spectators produced in a nuclear collision is maximal in the central rapidity region. Another effect must still be present which we will discuss below.

It is interesting to note that the coalescence of valence quarks which are co-moving with heavy quarks can play a role in explaining the leading particle effects seen in high x_F heavy meson and baryon production. This is analogous to the strong final state distortion effects one sees in Bethe-Heitler pair production $\gamma Z \rightarrow e^+e^-Z$ when the electron has low relative velocity with the final state nucleus. This is discussed in detail in Ref. 84.

Coherent Hadronization

The QCD capture reaction $\bar{q}b \rightarrow Bg$ is a fundamental process which should occur in the final stages of heavy quark jet hadronization. This reaction is analogous to the reaction $e^-p \rightarrow H\gamma$ in QED. In the atomic physics case, one can greatly increase the probability of capture by bathing the reaction in coherent light of the same frequency as that of the outgoing photon. Thus, in the nuclear case one may also be able to coherently induce hadronization of heavy quark capture reactions due to the presence of coherent co-moving gluons and hadrons.

The signal for coherent enhancement of the induced hadronization would be a non-linear dependence of the capture process (and consequent quarkonium suppression) with increasing associated multiplicity.

Intrinsic Charm and the Nuclear Suppression of Quarkonium

As emphasized above, the mechanisms previously discussed cannot readily account for the fact that the J/ψ cross section becomes increasingly suppressed as x_F increases. In fact, as emphasized by NA3²⁶, there is even a more serious incompatibility with the standard gluon-fusion picture of heavy quark production: the shape of the J/ψ production at large x_F is too hard if one assumes the standard $(1-x)^5$ counting rule form for the gluon distribution in protons and pions. The possibility that the gluon distribution itself could be much harder than assumed in standard models is unlikely due to the successful fits to $\gamma p \rightarrow J/\psi X$ data.

A natural explanation of the increase of the nuclear suppression in J/ψ production with x_F is provided by the existence of two production mechanisms, the extrinsic and intrinsic ones.⁸⁵ As discussed above, intrinsic charm production is suppressed by a factor $1/m_c^2$, but this mechanism can still dominate the small gluon fusion cross section at large x_F . Since the intrinsic heavy quark state tends to have a larger transverse size than the extrinsic one, it will suffer more rescattering in the nucleus. The x_F -dependence of α can then be understood as reflecting the increasing importance of intrinsic Fock states at large x_F . A comprehensive treatment of these effects as well as the suppression of charmonium production at low x_F due to co-moving spectators is given in Ref. 30. A short discussion of this work is given in the next section.

SYSTEMATICS OF J/ψ PRODUCTION IN NUCLEAR COLLISIONS³⁰

Recently Ramona Vogt, Paul Hoyer, and I³⁰ have presented a comprehensive QCD-based model for the x_F and nuclear dependence of heavy quarkonium production in photon-, hadron-, and nuclear-induced collisions. The x_F dependence calculated in the model reflects both leading-twist QCD fusion subprocesses and higher-twist intrinsic heavy-quark components of the hadron wavefunction. The

model includes A -dependent effects due to final-state absorption, interactions with co-movers, shadowing of parton distributions, as well as the intrinsic heavy-quark components. The various effects are identified by comparisons with data for J/ψ , ψ' , and T production in pion-, proton-, and nucleus-nucleus collisions.

As in the analysis of NA3,²⁶ we assume the existence of two production components in order to explain the x_F dependence heavy quarkonium production. The first component, dominant at small to moderate values of x_F , is the perturbative QCD model of parton fusion.³⁸ To first approximation, this hard-scattering approach predicts a linear A dependence, as in lepton pair production by the Drell-Yan mechanism. Some absorption of the hadronic system can occur, leading to a less than linear A dependence of J/ψ production by parton fusion. In addition, several initial and final state effects contribute to the A dependence of parton fusion in the model, particularly the interactions of the heavy quarks with co-moving spectators and the nuclear shadowing or anti-shadowing of the target gluons and sea quarks.

In the model, the probability for the charm quarks to survive co-mover interactions to produce a charmonium state is given by

$$S(b) = \exp - \int_{\tau_0}^{\tau_f} d\tau (\sigma_{co} v) n(\tau, b) , \quad (43)$$

where σ_{co} is the -co-mover absorption cross section, $v \sim 0.6$ is the relative velocity of the charm quarks with the co-movers, and $n(\tau, b)$ is the density of co-movers at time τ and impact parameter b . The integration extends from the time τ_0 , when the co-moving secondaries are formed, until τ_f , the proper lifetime over which the co-movers can interact with the charm quarks. In the case of heavy ion collisions the rapidity density of co-movers increases with E_T , the global transverse energy. One then finds that in order to be compatible with the observed values of

$$Y(E_T) = (d\sigma(A_1 A_2 \rightarrow J/\psi X) / dE_T) / (d\sigma(A_1 A_2 \rightarrow \mu^+ \mu^-) / dE_T)$$

in the NA38²⁹ experiment, one needs $(\sigma_{co} v) \sim 1.2 \text{ mb}$. (See Fig. 16). Similarly, the nuclear suppression of the total T production cross section seen in the

E772 800 GeV pA experiment can be accounted for if there is no strong flavor dependence of the co-mover cross section. (See Fig. 17). The suppression of Υ production observed at negative x_F also appears to be accounted for by the co-mover interactions.

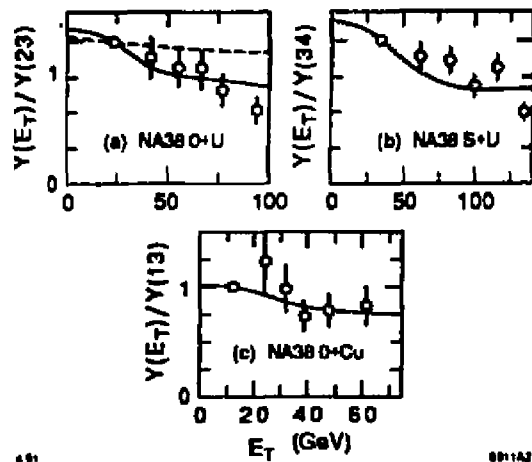


Figure 16. The effective co-mover cross section is fixed at $\sigma_{co} = 2$ mb from an examination of the NA38 (a) O+U, (b) S+U, and (c) O+Cu J/ψ production data at $\sqrt{s} = 19.4$ GeV.⁸⁶ The calculation with $\sigma_{co} = 0$ is shown as a dashed line in figure (a). (From Ref. 30.)

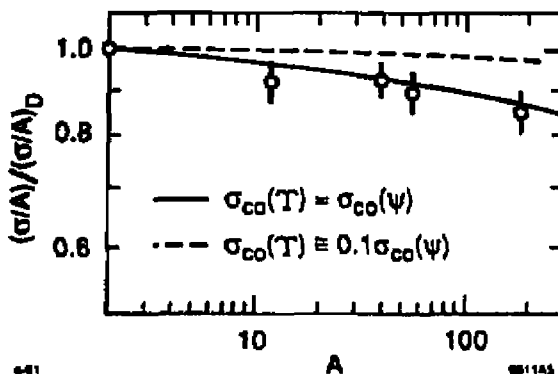


Figure 17. The A dependence of Υ production as determined by E772.⁸⁷ Results are shown for two assumptions for $\sigma_{co}(T)$. The first, $\sigma_{co}(T) = \sigma_{co}(W)$, is shown in the solid curve, and the second, $\sigma_{co}(T) = \sigma_{co}(W)(m_c/m_b)^2$, is given by the dashed curve.

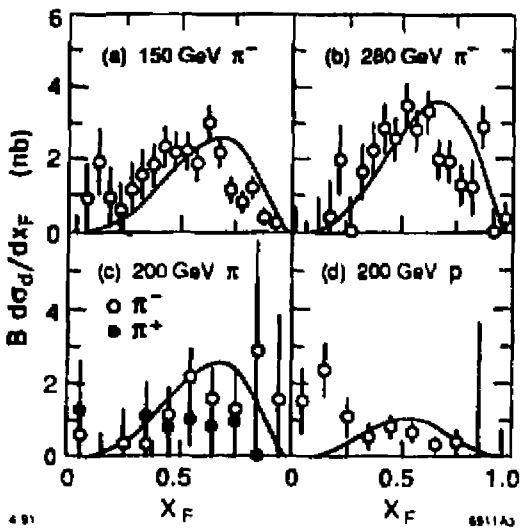


Figure 18. The NA3 data for the “dissociative” or “ $A^{2/3}$ ” component $B d\sigma_d/dx_F$ for ψ production on nuclear targets is compared with predictions based on the intrinsic charm x_F distributions in p and π projectiles as given in Eqs. (37) and (38) of Ref 30. Figures (a), (b), and (c) are from the π data at 150, 280, and 200 GeV respectively, Figure (d) compares the p beam data at 200 GeV with the calculation.

The second component of the x_F dependence is assumed to arise from an intrinsic heavy quark component of the projectile.^{13,85} Since the charm quark mass is large, these quarks carry a significant fraction of the longitudinal momentum, contributing to the large x_F portion of the cross section. In this picture, the intrinsic $c\bar{c}$ state is of small spatial extent and passes through the target while the slower light quarks interact primarily on the nuclear surface, giving rise to a near $A^{2/3}$ dependence of intrinsic charm. The comparison of the predictions of the model for intrinsic charm with the non-fusion “dissociative” component of the NA3 data is shown in Fig. 18. A comparison with the nuclear dependence of the total J/ψ data in πA and $p A$ collisions is shown in Fig. 19.

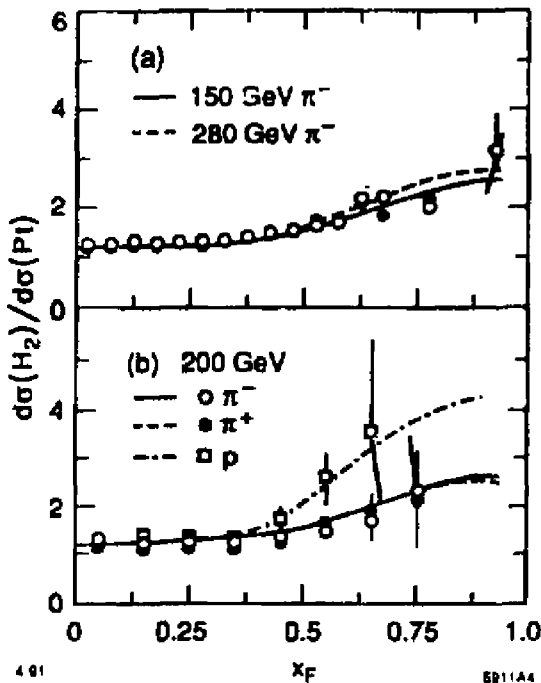


Figure 19. The nuclear x_F -dependence of J/ψ production from NA3²⁶. Figure (a) compares the model of Ref. 30 with π^- induced J/ψ production at 150 GeV (solid curve) and 280 GeV (dashed curve). Figure (b) compares 200 GeV J/ψ production by π^- (solid curve), π^+ (dashed curve), and p (dot-dashed curve) beams with the calculations.

Predictions for Heavy Quarkonium Production at RHIC

Vogt, Hoyer, and I have also used our model³⁰ to predict the behavior of quarkonium production at RHIC, the heavy-ion collider to be built at Brookhaven. These calculations may serve as a benchmark against which the future data can be compared in a search for new effects. Fig. 20(a) shows the predicted A dependence in 100 GeV on 100 GeV pA collisions. We first present the A dependence of the J/ψ production cross section. At $\tau = m_\psi/\sqrt{s} = 0.015$ and $x_F = 0$, the nuclear shadowing contribution is quite important, large enough to be experimentally confirmed or ruled out. The solid curve shows the full result whereas the dashed curve shows the prediction of the model leaving out gluon shadowing. There is a 25% difference in σ/A with and without shadowing at high A . (The ψ' results are similar.) We also show predictions for Υ production in pA collisions

It is clear that all of the above A dependent effects must be considered in a complete QCD description of J/ψ and Υ production. All the contributions we have examined in our model will be present in the 'background' of ultra-relativistic heavy-ion collisions. In particular, it is necessary to understand J/ψ production in detail to search for exotic effects such as quark-gluon plasma production.

The present experimental evidence for the existence of intrinsic charm in hadronic and nuclear collisions must still be regarded as suggestive but not conclusive. More quantitative studies of the intrinsic charm wavefunction, using multiparton distributions, coupled with better data on open charm at large x_F is clearly needed. Electroproduction studies can play a definitive role by measuring the charm structure function in semi-inclusive reactions, and by measuring the distribution of charmed hadrons and charmonium in the large x_F proton fragmentation region.

COLOR TRANSPARENCY

One of the most interesting QCD phenomena that can be tested in nuclei is "color transparency."^{30,31} A basic feature of perturbative QCD is the assertion that a hadron can only scatter through large momentum transfer and stay intact if its wavefunction is in a fluctuation²⁰ which contains only valence quarks at small transverse separation $b_\perp \sim 1/Q$. QCD then makes the remarkable prediction that the cross section for large momentum transfer quasi-elastic scattering such as $e p \rightarrow e p$ in a nucleus will be unaffected by final-state absorption corrections, since the scattering is dominated by a configuration of the valence-quark wavefunction of the proton which has a small color dipole moment. (By definition, quasi-elastic processes are nearly coplanar, integrated over the Fermi motion of the protons in the nucleus. Such processes are nearly exclusive in the sense that no extra hadrons are allowed in the final state.) Thus, at large momentum transfer and energies, quasi-elastic exclusive reactions are predicted to occur uniformly in the nuclear volume, unaffected by initial or final state multiple-scattering or absorption of the interacting hadrons. This remarkable phenomenon is called color transparency, reflecting the transparency of the nucleus to small color-singlet configurations. As

emphasized by Pire and Ralston,⁸⁹ the nucleus filters out the non-perturbative soft-contributions.

There are two conditions which set the kinematic scale where PQCD color transparency should be evident and for which quasi-elastic scattering cross section will be additive in the proton number Z of the nuclear target. First, the hard scattering subprocess must occur at a sufficiently large momentum transfer so that only small transverse size wavefunction components $\psi(r_1, b_\perp \sim 1/Q)$ with small color dipole moments dominate the reaction. Second, the state must remain small during its transit through the nucleus. The expansion distance is controlled by the time in which the small Fock component mixes with other Fock components. By Lorentz invariance, the time scale $\tau = 2E_p/\Delta M^2$ grows linearly with the energy of the hadron in the nuclear rest frame, where ΔM^2 is the difference of invariant mass squared of the Fock components. The scale in momentum transfer that sets the onset of color transparency reflects the coherent formation time.^{90,91} The first test of this phenomenon in electroproduction will be the NE-18 $eA \rightarrow ep$ ($A = 1$) two-arm coincidence test using the 9 GeV NPAS injector at SLAC.⁹²

More generally, it is possible to use a nucleus as a "color filter"^{93,89} to separate and identify the threshold and perturbative contributions to the scattering amplitude. If the interactions of an incident hadron are controlled by gluon exchange, then the nucleus will be transparent to those fluctuations of the incident hadron wavefunction which have small transverse size. Such Fock components have a small color dipole moment and thus will interact weakly in the nucleus; conversely, Fock components with slow-moving massive quarks cannot remain compact. They will interact strongly and be absorbed during their passage through the nucleus.

The only existing test of color transparency is the measurement of quasi-elastic large angle pp scattering in nuclei at Brookhaven.²³ The transparency ratio is observed to increase as the momentum transfer increases, in agreement with the color transparency prediction. However, in contradiction to perturbative QCD expectations, the data suggests, surprisingly, that normal Glauber absorption seems to recur at the highest energies of the experiment $p_{lab} \sim 12$ GeV/c. Even more striking is that this is the same energy at which the spin correlation A_{NN}

is observed to rise sharply to $A_{NN} \simeq 0.6$;²⁴ i.e. the cross section for protons scattering with their spins parallel and normal to the scattering plane becomes four times the cross section for anti-parallel scattering, which is again in strong contradiction to PQCD expectations.

The Charm Threshold

It is important to note²³ that the breakdown of color transparency and the onset of strong spin-spin correlations both occur at $\sqrt{s} \sim 5 \text{ GeV}$ or $p_{\text{lab}} \sim 12 \text{ GeV}/c$, which is just where the charm threshold occurs in pp collisions. At this energy the charm quarks are produced at rest in the center of mass, and all of the eight quarks have zero relative velocity. The eight-quark cluster thus moves through the nuclear volume with just the center-of-mass velocity. Even though the initial cluster size is small (since all valence quarks had to be at short transverse distances to exchange their momenta), the multi-quark nature and slow speed of the cluster implies that it will expand rapidly and be strongly absorbed in the nucleus. This Fock component will then not contribute to the large-angle quasi-elastic pp scattering in the nucleus: it will be filtered out.

The charm threshold effect will couple most strongly to the $J = L = S = 1$ partial wave in pp scattering.²³ (The orbital angular momentum of the pp state must be odd since the charm and anti-charm quarks have opposite parity.) This partial wave predicts maximal spin correlation in A_{NN} . Thus, if this threshold contribution to the $pp \rightarrow pp$ amplitude dominates the valence quark QCD amplitude, one can understand both the large spin correlation and the breakdown of color transparency at energies close to charm threshold. Thus the nucleus acts as a filter, absorbing the threshold contribution to elastic pp scattering, while allowing the hard scattering perturbative QCD processes to occur additively throughout the nuclear volume.⁸⁹ Experimentally, a strong enhancement of A_{NN} is observed at the threshold for strange particle production, which is again consistent with the dominance of the $J = L = S = 1$ partial wave helicity amplitude. (See Fig. 21.) The large size of A_{NN} observed at both the charm and strange thresholds is striking evidence of a strong effect on elastic amplitudes due to threshold production of fermion-antifermion pairs.

If the above explanation of the A_{NN} and color transparency anomalies is

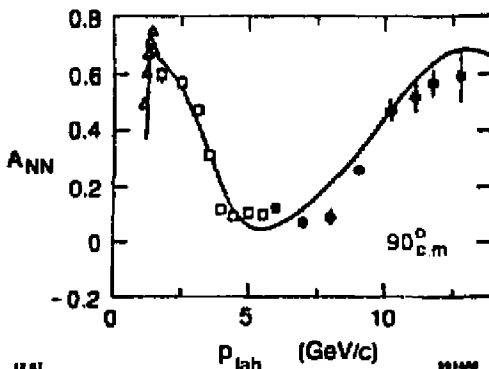


Figure 21. The spin-spin asymmetry A_{NN} in pp elastic scattering as a function of p_{lab} at $\theta_{cm} = \pi/2$. The data⁵⁴ are from Crosbie *et al.* (solid dots), Lin *et al.* (open squares) and Bhatia *et al.* (open triangles). The peak at $p_{lab} = 1.28$ GeV/c corresponds to the $p\Delta$ threshold. The data are well reproduced by the interference of the broad resonant structures at the strange ($p_{lab} = 2.35$ GeV/c) and charm ($p_{lab} = 12.8$ GeV/c) thresholds, interfering with a PQCD background. The value of A_{NN} from PQCD alone is 1/3. (From Ref. 23.)

correct, then one can identify the effect of heavy quark thresholds in hadron collisions by studying their elastic scattering at large angles. Through unitarity, even a nearly isotropic threshold cross section of only $1 \mu b$ for the production of open charm in pp collisions will have a profound influence on the $pp \rightarrow pp$ scattering at $\sqrt{s} \sim 5$ GeV because of its very small cross section at 90° . The production of charm at threshold implies that there is a contribution with massive, slow-moving constituents to the pp elastic amplitude which can modify the ordinary PQCD predictions, including dimensional counting scaling laws, helicity dependence, angular dependence, and especially the "color transparency" of quasi-elastic pp scattering in a nuclear target. Note that this effect would not affect the onset of color transparency in quasi-elastic ep scattering, but it could appear in other color transparency tests in electroproduction such as $eA \rightarrow e'\pi n(A-1)$.

There are many possible tests of color transparency in electroproduction, photoproduction and hadron production in nuclei. In each case one tests for the dominance of small components of the hadronic wavefunction in a hard-scattering exclusive reaction. In the case of high energy J/ψ or Υ photoproduction, the initially formed $Q\bar{Q}$ state can propagate freely through the nucleus as a small color-singlet forming the quarkonium state outside of the nucleus.⁶⁸ Detailed

quantum mechanical analyses of the evolution of such systems have recently been given in Ref. 90.

Nuclear-Bound Quarkonium

I have argued above that the breakdown of color transparency and the sharp increase of the spin-spin correlation A_{NN} in large angle $pp \rightarrow pp$ scattering at $\sqrt{s} \sim 5$ GeV reflects the onset of charm production in the inelastic channels. More generally, one can expect that any heavy quark system produced near threshold on a hadronic target will experience strong final state interactions, since there is a long time for the system to interact strongly. For example, there should be enhancements in the cross section to produce both open charm and charmonium in electroproduction at threshold beyond that expected from photon-gluon fusion due to both initial state intrinsic charm components in the wavefunction, and multi-gluon exchange interactions in the final state. The situation could be even more interesting in a nuclear target.

For example, consider the reaction $\gamma^* {}^3He \rightarrow {}^3He(c\bar{c})$ where the charmonium state is produced nearly at rest. At the threshold for charm production, the produced particles will be slow (in the center of mass frame) and will fuse into a compound nucleus because of the strong attractive nuclear force. The charmonium state will be attracted to the nucleus by the QCD gluonic van der Waals force. One thus expects strong final state interactions near threshold. In fact, it is argued in Ref. 22 that the $c\bar{c}$ system could bind to the 3He nucleus. It is thus possible that a new type of exotic nuclear bound state will be formed: charmonium bound to nuclear matter. Such a state should be observable at a distinct $\gamma^* {}^3He$ center of mass energy, spread by the width of the charmonium state, and it will decay to unique signatures. The binding energy in the nucleus gives a measure of the charmonium's interactions with ordinary hadrons and nuclei; its hadronic decays will measure hadron-nucleus interactions and test color transparency starting from a unique initial state condition.

In QCD, the nuclear forces are identified with the residual strong color interactions due to quark interchange and multiple gluon exchange. Because of the identity of the quark constituents of nucleons, a short-range repulsive component is also present (Pauli blocking). From this perspective, the study of heavy

quarkonium interactions in nuclear matter is particularly interesting; due to the distinct flavors of the quarks involved in the quarkonium-nucleon interaction, there is no quark exchange to first order in elastic processes, and thus no one-meson-exchange potential from which to build a standard nuclear potential. For the same reason, there is no Pauli-blocking and consequently no short-range nuclear repulsion. The nuclear interaction in this case is purely gluonic and thus of a different nature from the usual nuclear forces.

The production of nuclear-bound quarkonium would be the first realization of hadronic nuclei with exotic components bound by a purely gluonic potential. Furthermore, the charmonium-nucleon interaction would provide the dynamical basis for understanding the spin-spin correlation anomaly in high energy $p\bar{p}$ elastic scattering.²³ In this case, the interaction is not strong enough to produce a bound state, but it can provide an enhancement at the heavy-quark threshold characteristic of an almost-bound system. The signal for the production of almost-bound nucleon (or nuclear) charmonium systems near threshold is the isotropic production of the recoil nucleon (or nucleus) at large invariant mass $M_X \simeq M_\eta$. The experimental prospects for studying the formation of nuclear bound charmonium in anti-proton nucleus collisions are discussed by Seth in his contribution to these proceedings.⁹⁵

CONCLUSIONS

In these lectures, I have shown how studies of the production and decay of heavy quark systems allow us to probe QCD in extraordinary ways not possible in ordinary hadrons. A number of novel heavy-quark phenomena predicted by QCD are just now beginning to be explored, such as color transparency, nuclear-bound quarkonium, intrinsic charm and beauty, and enhancements due to heavy-quark thresholds. Several intriguing effects appear important for understanding the observed suppression of heavy quark and quarkonium production in nuclear collisions, including gluon shadowing, the peripheral excitation of intrinsic heavy quark components of hadron wavefunctions, and the “induced hadronization” due to the coalescence of heavy quarks with co-moving spectators. The study of these topics should lead to new insights into the mechanisms for jet hadronization, color

confinement, the structure of hadronic wavefunctions, and other non-perturbative QCD phenomena. I have particularly emphasized the impact of intrinsic charm and beauty distributions for the production of high momentum heavy particles in ep pp and heavy ion colliders, including the production of quarkonium at high x_F in the proton fragmentation region at HERA. On the theoretical side, I have discussed the utility of effective Lagrangian techniques and light-cone Fock-state expansions for separating perturbative and non-perturbative QCD phenomena in heavy quark systems. An important application of this analysis is a new form of QCD amplitude factorization for calculating the decay of B -mesons to light hadrons.

ACKNOWLEDGEMENTS

Much of the material presented in these lectures is based on collaborations with Ernest Henley, Kent Hornbostel, Paul Hoyer, Peter Lepage, Al Mueller, Ivan Schmidt, Adam Szczepaniak, Guy de Teramond, and Ramona Vogt. I want to particularly thank Paul Hoyer for many valuable discussions and suggestions. I also wish to thank Professors Campbell, Kamal, and Khanna for their work in organizing an outstanding Winter Institute at Lake Louise.

REFERENCES

1. J. H. Kuhn and P.M. Zerwas, Phys. Rept. 167, 321 (1988).
2. The CDF Collaboration (F. Abe, et al.), Phys. Rev. D43 664 (1991).
3. R. L. Jaffe, Phys. Lett. B245, 221-228 (1990).
4. S. Gupta and H. Quinn, Phys. Rev. D25, 838 (1982).
5. N. Isgur, APS talk, (1991) unpublished.
6. A convenient expression for the quark interchange amplitude in terms of light-cone wavefunctions is given in J. F. Gunion, S. J. Brodsky, R. Blankenbecler, Phys. Rev. D8, 287 (1973); Phys. Lett. 39B, 649 (1972).
7. V. N. Gribov, Physica Scripta T15, 164 (1987).
8. B. Mele and P. Nason, CERN-TH-5972-90 (1990), and references therein.

9. P. Burrows, V. Del Duca, and P. Hoyer, SLAC-PUB (1991), to be published.
10. G. P. Lepage and B. A. Thacker, CLNS-87/114, (1987). See also G. P. Lepage and W. Caswell, Phys. Lett. 167B, 437 (1986).
11. N. Isgur and M. B. Wise, Phys. Rev. Lett. 66, 1130 (1991). M. B. Wise, these proceedings.
12. J.D. Bjorken, SLAC-PUB-5362, (1990). Adam F. Falk, H. Georgi, B. Grinstein, M. B. Wise, Nucl. Phys. B343, 1-13 (1990).
13. S. J. Brodsky, P. Hoyer, C. Peterson, and N. Sakai, Phys. Lett. 93B, 451 (1980); S. J. Brodsky, C. Peterson, and N. Sakai, Phys. Rev. D23, 2745 (1981).
14. S. J. Brodsky, P. Hoyer, A. H. Mueller, to be published.
15. Bjorken has particularly emphasized the need to study large x_F physics at the new colliders. J.D. Bjorken (SLAC), SLAC-PUBS-5361,5362, (1990), and to be published.
16. P. Hoyer and S. J. Brodsky, SLAC-PUB-5374 (1990).
17. S. J. Brodsky, G. P. Lepage, and P. B. Mackenzie Phys. Rev. D28, 228 (1983). For a recent discussion of the scale-fixing problem in QCD, see J. C. Collins, ANL-HEP-CP-90-58 (1990).
18. S. J. Brodsky, D. G. Coyne, T. A. DeGrand, and R. R. Horgan, Phys. Lett. 73B, 203 (1978).
19. For reviews and references, see the proceedings of the *DESY Topical Meeting: Small x Behavior of Deep Inelastic Structure Functions in QCD*. Hamburg, Germany, (1990), published in the *Proceedings Supplements of Nuclear Physics B*. (1991).
20. G. P. Lepage and S. J. Brodsky, Phys. Rev. D22, 2157 (1980); Phys. Lett. 87B, 359 (1979); Phys. Rev. Lett. 43, 545, 1625(E) (1979).
21. A. Szczepaniak, E. M. Henley, S. J. Brodsky, Phys. Lett. B243, 287 (1990).
22. S. J. Brodsky, G. de Teramond, and J. Schmidt, Phys. Rev. Lett. 64, 1011 (1990).
23. S. J. Brodsky and G. de Teramond, Phys. Rev. Lett. 60, 1924 (1988).
24. G. R. Court, et al., Phys. Rev. Lett. 57, 507 (1986).

25. A. S. Carroll, et al., *Phys. Rev. Lett.* **61**, 1698 (1988).
26. J. Badié et al., *Z. Phys.* **C20**, 101 (1983).
27. P. Hoyer, M. Vänttinen and U. Sukhatme, *Phys. Lett.* **246B**, 217 (1990).
28. D. M. Alde, et al., *Phys. Rev. Lett.* **64**, 2479 (1990) and Los Alamos preprint LA-UR-90-2331 (1990); C. S. Mishra, et al., Contribution to the XXVth Rencontres de Moriond, Les Arcs (1990), Fermilab-Conf-90/100-E (May 1990).
29. M. C. Abreu, et al., *Z. Phys.* **C38** 117 (1988).
30. R. Vogt, S. J. Brodsky, and P. Hoyer, SLAC-PUB 5421 (1991). (To be published in *Nuclear Physics B*.)
31. S. J. Brodsky and A. H. Mueller, *Phys. Lett.* **206B**, 685 (1988), and references therein.
32. G. P. Lepage, S. J. Brodsky, T. Huang, and P. Mackenzie, published in the *Proceedings of the Banff Summer Institute* (1981).
33. The Dirac approach with a confining potential has been utilized by R. R. Mendel and H. D. Trottier, *Phys. Lett.* **B231**, 620 (1989), and refs. therein. A single-time relativistic equation for heavy-light mesons analogous to the Salpeter equation has been proposed for heavy mesons by X. Q. Zhu and F. C. Khanna, these proceedings. I thank Profs. Mendel and Khanna for helpful conversation regarding this work.
34. For a review see, D. R. Yennie, *Brandeis Summer Institute in Theoretical Physics Lectures*, Vol. I (1963).
35. For a review of exclusive processes in QCD, and references see S. J. Brodsky, and G. P. Lepage, published in *Perturbative Quantum Chromodynamics*, Edited by A. H. Mueller, World Scientific (1989).
36. S. J. Brodsky and G. P. Lepage, *Phys. Rev.* **D24** 2848 (1981).
37. S. J. Brodsky, J. G. Gunion, and M. Scadron, unpublished.
38. P. A. M. Dirac, *Rev. Mod. Phys.* **21**, 392 (1949).
39. K. Hornbostel, S. J. Brodsky, and H. C. Pauli, *Phys. Rev.* **D41** 3814, (1990). A. C. Tang, S. J. Brodsky, and H. C. Pauli, SLAC-PUB-5425 (1991); and references therein.

40. S. D. Drell and T. M. Yan, *Phys. Rev. Lett.* **24**, 181 (1970).
41. S. J. Brodsky and S. D. Drell, *Phys. Rev. D***22**, 2236 (1980).
42. General QCD analyses of exclusive processes are given in Ref. 20, S. J. Brodsky and G. P. Lepage, SLAC-PUB-2294, presented at the Workshop on Current Topics in High Energy Physics, Cal Tech (Feb. 1979), S. J. Brodsky, in the *Proceedings of the La Jolla Institute Summer Workshop on QCD*, La Jolla (1978), A. V. Efremov and A. V. Radyushkin, *Phys. Lett.* **89A**, 245 (1980), V. L. Chernyak, V. G. Serbo, and A. R. Zhitnitskii, *Yad. Fiz.* **31**, 1069 (1980), S. J. Brodsky, Y. Frishman, G. P. Lepage, and C. Sachrajda, *Phys. Lett.* **91B**, 239 (1980), and A. Duncan and A. H. Mueller, *Phys. Rev. D***21**, 1636 (1980).
43. QCD predictions for the pion form factor at asymptotic Q^2 were first obtained by V. L. Chernyak, A. R. Zhitnitskii, and V. G. Serbo, *JETP Lett.* **26**, 594 (1977), D. R. Jackson, Ph.D. Thesis, Cal Tech (1977), and G. Farrar and D. Jackson, *Phys. Rev. Lett.* **43**, 246 (1979). See also A. M. Polyakov, *Proceedings of the International Symposium on Lepton and Photon Interactions at High Energies*, Stanford (1975), and G. Parisi, *Phys. Lett.* **84B**, 225 (1979). See also S. J. Brodsky and G. P. Lepage, in *High Energy Physics-1980*, proceedings of the XXth International Conference, Madison, Wisconsin, edited by L. Durand and L. G. Pondrom (AIP, New York, 1981); p. 568. A. V. Efremov and A. V. Radyushkin, *Rev. Nuovo Cimento* **3**, 1 (1980); *Phys. Lett.* **94B**, 245 (1980). V. L. Chernyak and A. R. Zhitnitsky, *JETP Lett.* **25**, 11 (1977); G. Parisi, *Phys. Lett.* **43**, 246 (1979); M. K. Chase, *Nucl. Phys.* **B167**, 125 (1980).
44. N. Isgur and C. H. Llewellyn Smith, *Phys. Lett.* **B217**, 535 (1989).
45. V. L. Chernyak, A.R. Zhitnitskii, *Phys. Rept.* **112**, 173 (1984). See also M. Gari and N. G. Stephanis, *Phys. Lett.* **B175**, 462 (1986), and references therein.
46. J. Hansper, R. Eckardt, and M. F. Gari *et al.*, Ruhr-Universität Bochum preprint (1991).
47. A. Szczepaniak, L. Mankiewicz Univ. of Florida Preprint (1991).
48. J. Botts, *Nucl. Phys.* **B353** 20 (1991).

49. P. V. Landshoff, Phys. Rev. D10, 1024 (1974).
50. P. Stoler, Phys. Rev. Lett. 66, 1003 (1991); and to be published in Phys. Rev. D.
51. C. E. Carlson and J. L. Poor, Phys. Rev. D38, 2758 (1988).
52. W. Kwong, P. B. Mackenzie, R. Rosenfeld, and J. L. Rosner Phys. Rev. D37, 3210, (1988).
53. W.-S. Hou and A. Soni, Phys. Rev. Lett. 59, 569, (1983). S. J. Brodsky, G. P. Lepage, and S. F. Tuan, Phys. Rev. Lett. 59, 621 (1987).
54. M. Anselmino, M. Genovese, and E. Predazzi, University of Torino preprint, (1990).
55. S. J. Brodsky, G. P. Lepage and S. A. A. Zaidi, Phys. Rev. D23, 1152 (1981).
56. D. Bartoletta *et al.*, Phys. Rev. Lett. 62, 2436 (1989).
57. R. K. Ellis, FERMILAB-PUB-91-30-T, (1991).
58. V. Barger, W. Y. Keung, and R. N. Phillips, Phys. Lett. 91B, 253 (1980).
59. G. T. Bodwin, S. J. Brodsky, G. P. Lepage, Phys. Rev. D39, 3287 (1989).
60. John C. Collins, D. E. Soper, G. Sterman, published in *Perturbative QCD* edited by A.H. Mueller, World Scientific, (1989).
61. Phys. Rev. D31 2616, (1985). D34 3932, (1986E).
62. Jian-wei Qiu, G. Sterman, Nucl. Phys. B353 105, 137 (1991).
63. P. Nason, S. Dawson, and R.K. Ellis, Nucl. Phys. B327 49 (1989).
64. W. Beenakker, W. L. van Neerven, R. Meng, G.A. Schuler and J. Smith, Stony Brook preprint ITP-SB-90-46, (1990).
65. For a recent discussion and further references, see C. S. Kim, Nucl. Phys. B353, 87 (1991).
66. J. J. Aubert, *et al.*, Nucl. Phys. B213, 31 (1983). See also E. Hoffmann and R. Moore, Z. Phys. C20, 71 (1983).
67. K. Hornbostel, private communication; S. J. Brodsky and K. Hornbostel, to be published.
68. S. J. Brodsky and I. A. Schmidt, Phys. Rev. D43, 179 (1991).

69. S. J. Brodsky, H. E. Haber, and J. F. Gunion, in *Anti-pp Options for the Supercollider*, Division of Particles and Fields Workshop, Chicago, IL, 1984, edited by J. E. Pilcher and A. R. White (SSC-ANL Report No. 84/01/13, Argonne, IL, 1984), p. 100; S. J. Brodsky, J. C. Collins, S. D. Ellis, J. F. Gunion, and A. H. Mueller, published in *Snowmass Summer Study 1984*, p. 227.

70. C. Peterson, D. Schlatter, I. Schmitt and P. M. Zerwas, *Phys. Rev. D27*, 105 (1983).

71. R. J. Cashmore, *Proceedings of the International Symposium on Production and Decay of Heavy Flavors*, Stanford (1987) (E. Bloom and A. Freidman, Eds.), p.118.

72. A. Kernan and G. VanDalen, *Phys. Rep.* 106, 297 (1984), and references therein.

73. S. P. K. Tavernier, *Rep. Prog. Phys.* 50, 1439 (1987); U. Gasparini, *Proceedings of the XXIV International Conference on High Energy Physics*, (R. Kotthaus and J. H. Kühn, Eds., Springer 1989), p. 971.

74. S. F. Biagi, *et al.*, *Z. Phys.* C28, 175 (1985); P. Chauvat, *et al.*, *Phys. Lett.* 199B, 304 (1987); P. Coteus, *et al.*, *Phys. Rev. Lett.* 59, 1530 (1987); C. Shipbaugh, *et al.*, *Phys. Rev. Lett.* 60, 2117 (1988); M. Aguilar-Benitez, *et al.*, *Z. Phys.* C40, 321 (1988).

75. M. Aguilar-Benitez, *et al.*, *Phys. Lett.* 161B, 400 (1985) and *Z. Phys.* C31, 491 (1986); S. Barlag, *et al.*, *Z. Phys.* C39, 451 (1988) and CERN-PPE/90-145 (1990).

76. M. MacDermott and S. Reucroft, *Phys. Lett.* 184B, 108 (1987); H. Cobbaert, *et al.*, *Phys. Lett.* 191B, 456 (1987), *ibid.*, 206B, 546 (1988) and *Z. Phys.* C36, 577 (1987); M. E. Duffy, *et al.*, *Phys. Rev. Lett.* 55, 1816 (1985); M. I. Adamovich, *et al.*, CERN-EP/89-123 (1989).

77. K. J. Anderson, *et al.*, *Phys. Rev. Lett.* 42, 944 (1979); A. S. Ito, *et al.*, *Phys. Rev. D23*, 604 (1981); J. Badier, *et al.*, *Phys. Lett.* 104B, 335 (1981); P. Bordalo, *et al.*, *Phys. Lett.* 193B, 368 (1987).

78. The final ISR results were reported by the R608 Collaboration (P. Chauvat, *et al.*), *Phys. Lett.* 199B 304, (1987).

79. Yu. M. Antipov, *et al.*, Phys. Lett. **76B**, 235 (1978); M. J. Corden, *et al.*, Phys. Lett. **110B**, 415 (1982); J. Badier, *et al.*, Z. Phys. **C20**, 101 (1983); S. Katsanevas, *et al.*, Phys. Rev. Lett. **60**, 2121 (1988).

80. S. J. Brodsky, H. J. Lu, Phys. Rev. Lett. **64**, 1342 (1990).

81. P. V. Landshoff, J. C. Polkinghorne, and R. D. Short, Nucl. Phys. **B28**, 210 (1970).

82. J. Qiu, Nucl. Phys. **B291** 746 (1987).

83. R. L. Anderson *et al.*, Phys. Rev. Lett. **38**, 262 (1977).

84. S. J. Brodsky, J. F. Gunion and D. E. Soper, Phys. Rev. **D36**, 2710 (1987).

85. S. J. Brodsky and P. Hoyer, Phys. Rev. Lett. **63**, 1566 (1989).

86. J.-Y. Grossiord *et al.*, Nucl. Phys. **A498**, 249 (1989).

87. J. Moss, in *proceedings of the VIIth International Conference on Ultrarelativistic Nucleus-Nucleus Collisions*, Menton, France, 1990, to be published in Nucl. Phys. **A**.

88. A. H. Mueller, *Proceedings of the XVII Recontre de Moriond* (1982); S. J. Brodsky, *Proceedings of the XIII International Symposium on Multiparticle Dynamics*, Volendam (1982).

89. J. P. Ralston and B. Pire, Phys. Rev. Lett. **61**, 1823 (1988), University of Kansas preprint 90-0548 (1990).

90. B. K. Jennings and G. A. Miller, Phys. Lett. **B236**, 209 (1990), and University of Washington preprint 40427-20-N90 (1990).

91. G. R. Farrar, H. Liu, L. L. Frankfurt, M. I. Strikman, Phys. Rev. Lett. **61**, 686 (1988). J. Hufner, B. Povh, and S. Gardner Phys. Lett. **B238**, 103 (1990).

92. For a recent review of color transparency phenomena, see L. L. Frankfurt and M. I. Strikman, Univ. of Illinois preprint (1991).

93. G. Bertsch, S. J. Brodsky, A. S. Goldhaber, and J. Gunion, Phys. Rev. Lett. **47**, 297 (1981).

94. T. S. Bhatia *et al.*, Phys. Rev. Lett. **49**, 1135 (1982); E. A. Crosbie *et al.*, Phys. Rev. **D23**, 600 (1981); A. Lin *et al.*, Phys. Lett. **74B**, 273 (1978); D. G. Crabb *et al.*, Phys. Rev. Lett. **41**, 1257 (1978); J. R. O'Fallon

et al., Phys. Rev. Lett. **39**, 733 (1977); For a review, see A. D. Krisch, UM-HE-86-39 (1987).

95. K. Seth, these proceedings.